PPE Distribution Planning and Capacity Acquisition During the COVID-19 Pandemic

by

Jordan Kiss

A thesis
presented to the University of Waterloo
in fulfillment of the
thesis requirement for the degree of
Master of Applied Science
in
Management Sciences

Waterloo, Ontario, Canada, 2021

© Jordan Kiss 2021

Author's Declaration

I hereby declare that I am the sole author of this thesis. This is a true copy of the thesis, including any required final revisions, as accepted by my examiners.

I understand that my thesis may be made electronically available to the public.

Abstract

The COVID-19 pandemic caused disruptions to global supply chains and the uncertainty surrounding its progression has created challenges in distributing critical supplies such as personal protective equipment (PPE). We consider the problem of distributing PPE during the COVID-19 pandemic by acquiring distribution and storage capacity from independent carriers for timely and efficiently delivery to health regions. First, a priority-based distribution model is presented that prioritizes health regions by pandemic severity where priorities are based on COVID-19 case counts. Then, we propose a two-stage stochastic model with recourse to examine PPE distribution with uncertain demand. In the first stage, capacity acquisition decisions are made along with an initial distribution plan. Once the pandemic severity unveils, changes to the distribution plan are made in the second stage. The stochastic model is solved using Benders decomposition and approximated using sample average approximation. Benders decomposition and sample average approximation produce similar results with an optimality gap of less than 1%. Benders decomposition requires about 20 minutes to solve, while sample average approximation requires almost an hour. We test on the Ontario health regions network and use the Ontario healthcare worker and COVID-19 data to predict future PPE demand using 1024 scenarios. Comparing the results with actual COVID-19 realizations, we found that the stochastic model provides sufficient PPE to satisfy demand at all regions. Furthermore, only minimum supply is rerouted in the second stage and existing inventory is used to satisfy demand increases where possible. When supply is more spread out amongst the regions, the proportion of demand received at high-priority regions is more balanced, and in the event of supply disturbances, distribution centres are used to stockpile PPE for time periods with low supply.

Acknowledgements

First, I would like to thank my supervisor, Professor Samir Elhedhli, for all his support and encouragement over the past two years. I'm thankful he took me on two years ago and agreed to be my supervisor. I appreciate all the time he has spent working with me and all the guidance he has provided. I've learned so much from him.

I would like to thank the readers of this thesis, Dr. Fatma Gzara and Dr. Joe Naoum-Sawaya for their invaluable comments and suggestions.

I would also like to thank my colleague, Paulo de Carvalho, for always being available when I needed technical help.

I am thankful for my parents, who have always been there for me and have always encouraged me along the way.

Table of Contents

List of Figures

List of Tables

Chapter 1

Introduction

The recent COVID-19 pandemic caused an increase in demand for personal protective equipment (PPE) around the world. PPE is critical for reducing the transmission of the virus and for protecting individuals who work in high-risk settings, such as healthcare workers (U.S. Food and Drug Administration, 2020). For many countries, including Canada, increased demand and insufficient stockpiles led to severe PPE shortages for healthcare workers and forced some healthcare workers to reuse single-use PPE (Warren, 2020). An observational study shows that front-line healthcare workers are at an increased risk of testing positive for COVID-19 and that having adequate supplies of PPE available is critical to protecting healthcare workers during large spikes in COVID-19 hospitalizations (Nguyen et al., 2020).

The process of reopening schools and businesses will also require an increase in demand for PPE (Flanagan, 2020). Many Canadian communities and businesses have adopted mandatory face mask laws (Chung, 2020) and are encouraging the use of hand sanitizer(Chiu, 2020). For example, the Ontario Government has mandated the use of masks in most non-residential indoor settings, such as schools (Ministry of Health, 2021). The

Ontario Ministry of Education has mandated that all students in Grades 1 to 12 must wear a mask and that all teachers and school staff must wear a medical-grade mask as well as eye protection when in the school building. (Ministry of Education, 2021). Such regulations emphasize the importance of quickly distributing PPE across the province.

Early on in the pandemic, several countries, including China, had export bans in place, restricting the global flow of PPE and raw materials. With about half of global pre-pandemic mask production located in China, such bans contributed to global supply shortages and disruptions (Park et al., 2020). Before the pandemic, having PPE stockpiles was seen as a poor business decision for both businesses and countries as they can be expensive to maintain (Feinmann, 2020). An audit of Canada's National Stockpile System in 2010 found that large proportions of Canada's existing stockpiled PPE supplies had expired and as of July 2020, had still not been adequately replaced (Laing and Westervelt, 2020). According to Collis and Ungerman (2020), the pandemic may influence how companies and governments operate in the future as societies will prioritize PPE stockpiles and robust global supply chains to prepare for another eventual pandemic. The safety of front-line healthcare workers, the safety of economic reopening, and preparation for another pandemic highlight the importance of robust supply chains for PPE distribution.

Governments around the world are pursuing other PPE supply options (Dyer, 2020) as the importance of having adequate PPE in COVID-19 hotspots is recognized. In response to the PPE shortage, the Government of Canada has established an online hub to connect buyers and sellers of PPE (Government of Canada, 2020b). The hub links PPE buyers to provincial and territorial directories of suppliers. The hub also provides access to a contingency supply of PPE to be used for essential service emergencies. For PPE sellers, the hub makes finished products and related materials available to buyers. The hub also provides product specifications and requirements for organizations that are beginning to

manufacture PPE to accommodate the increase in demand.

As Alicke et al. (2020) describe, companies and governments should review supply chain practices to better deal with the COVID-19 pandemic and to better prepare for future distribution interruptions. With increased PPE demand and dynamic supply, government distribution networks are at risk of being overwhelmed during the pandemic. To alleviate some of the pressure faced by public supply chains, governments can collaborate with private carriers. For example, Polygenis (2020) describes how public and private partnerships are used in some Canadian provinces to improve the distribution of the annual influenza vaccines. Integration between public and private supply chains allows for governments to ensure equitable vaccine distribution without having to invest in expanded supply chain infrastructure. Polygenis (2020) believes that similar partnerships will be required to provide all Canadians with access to COVID-19 vaccines due to the large number of vaccines needed and the vaccines' frozen storage requirements.

Collaborating with private carriers can help reduce the pandemic's impact on supply chains. Such collaborations can assist by increasing the speed and capacity of the distribution networks. For example, Fedex Express Canada and Innomar Strategies Inc. have partnered with the Government of Canada to provide warehouse capacity and transportation to provincial and territorial authorities to assist with vaccine distribution and administration (Government of Canada, 2020a). Similarly, the Government of Ontario has set up Supply Ontario (Ministry of Government and Consumer Services, 2021), which is an agency that allows the provincial government to purchase supplies as a single organization and ensures that supplies are available across the province. Supply Ontario works with partners in numerous sectors to avoid pandemic-related disruptions for PPE and other critical equipment as well as to have a long-term sustainable supply chain. Partnerships between governments and private carriers provide the dual goal of satisfying PPE demand

and providing economic benefit.

This work provides a set of models to distribute PPE under different conditions. The first model allows for distribution with sufficient supply and known demand. The second model considers PPE distribution with insufficient supply in which PPE must be prioritized by severity. The third model considers PPE distribution under uncertain PPE demand. We provide deterministic and stochastic programming models in which warehouse and transportation capacity can be acquired from independent carriers to assist with distribution. We consider PPE distribution in the events of supply shortages and with uncertain demand. The stochastic programming model is solved using Benders decomposition and approximated using sample average approximation.

The remainder of this thesis is as follows. A literature review is provided in Chapter 2. Chapter 3 describes the problem and the mathematical models used to solve the problem. Chapter 4 presents the data used to test the models. Numerical testing is given in Chapter 5 and conclusions are presented in Chapter 6.

Chapter 2

Literature Review

2.1 Supply Chain Responses to Humanitarian Crises

The COVID-19 pandemic has impacted supply chains around the world. Being a humanitarian crisis, we review the literature on supply chain responses to the COVID-19 pandemic as well as to previous humanitarian crises. Patel et al. (2017) review the PPE supply chain responses in the United States from the H1N1 and the Ebola outbreaks. The authors suggest many improvements including using commercial supply chains to distribute PPE stockpiles. Tomasini and Van Wassenhove (2009) and Cozzolino et al. (2017) use case studies to discuss the role that the private sector can have in humanitarian logistics such as providing distribution for assets during a crisis. Pettit and Beresford (2009) perform a detailed literature review on supply chain capacity increases due to the collaboration of commercial organizations during humanitarian crises. The authors describe how coordination of collaboration is much more difficult in the middle of a crisis than before a crisis and consider the applicability of ten supply chain critical success factors to humanitarian relief efforts. Jahre and Jensen (2010) conduct an interpretative case study on the use of

clusters and inter-cluster coordination to ensure that capacity is met during emergencies. Hoek (2020) conducts a review of news feeds, seminars, and interviews to identify research opportunities for more resilient supply chains. The author suggests creating decision models that consider global sourcing and model responsiveness instead of only cost. Such a model could be used for distribution of PPE to high-priority regions. Ivanov and Dolgui (2020) use an ecological model to argue that intertwined supply networks improve a supply chain's ability to survive and recover from challenging environments such as the COVID-19 pandemic. Rowan and Laffey (2020) use a case study to explore the efficacy of addressing the PPE supply chain shortage using reprocessing of products. Geng et al. (2020) propose an evolution model to reduce supply chain network vulnerability resulting from cascading failure. The authors use three classifications of supply chain criticality to balance efficiency and vulnerability. Case studies are used to illustrate how the model improves supply chain resilience.

Research has also been done in assessing the risk of viral transmission. Castro et al. (2017) use Zika virus transmission rates with a Markov branch process model to estimate the risk of Zika virus outbreaks in Texas. The authors use Poisson processes to model infections by transmission and by introduction rates to the region. Javan et al. (2020) use the framework provided by Castro et al. (2017) to estimate the COVID-19 risk for the United States by county.

We now review research on existing network models that are used for new product demand as we consider companies with available capacity being used for PPE distribution. Chauhan et al. (2004) develop an analytical tool for supply chain design that can be used to provide a strategy for new market opportunities by creating a heuristic approach to a mixed integer programming problem that incorporates the production and distribution of a new product in an existing supply chain. The problem is to select providers and

producers in a three-echelon system with deterministic demand. Nodes have limited production and transportation capacities, however capacity can be increased by introducing new resources. Similarly, Chauhan et al. (2006) develop a decomposition-based solution approach for a mixed integer linear programming problem that uses idle supply chain capacities for producing and transporting a new product with deterministic demand. Amini and Li (2011) develop a mixed-integer nonlinear programming problem for a similar situation and compared the results using seven heuristic policies for methods of product diffusion. The authors find that hybrid models, which consider both product manufacturing and distribution, outperform non-hybrid models. Pan and Nagi (2010) develop a similar mathematical model for the manufacturing and distribution of a new product with uncertain demand, where individual companies are selected for production and logistics nodes. A shortest path heuristic is developed to provide an upper bound. Brandenburg (2015) develop a mixed-integer linear programming model for supply chain design for a new product with uncertain demand that considers both environmental and economic factors. The author finds that decentralized supply chain designs enable carbon emission reduction without affecting supply chain performance and that by increasing the focus of economic optimization, demand uncertainties negatively impact the environmental impact.

2.2 Two-Stage Stochastic Programming with Recourse

Multi-stage stochastic programming has been studied extensively. Such stochastic models usually focus on making initial decisions, then modifying the decisions as new information becomes available. Bai et al. (2014) present a two-stage stochastic model to satisfy uncertain customer demand that allows for vehicle rerouting. In the first stage, the network is created without knowing customer demand. In the second stage, once demand is known,

additional trucks can be added or removed from routes to satisfy the demand. Zanjani et al. (2009) present a two-stage stochastic model with recourse for sawmill production planning. The authors use a hybrid scenario tree to account for demand and yield uncertainty. The amount production and inventory of product and raw material can be changed in the second stage as more information regarding yield and demand realizations becomes available. Özaltın et al. (2018) propose a bilevel multistage stochastic mixed integer program to maximize influenza vaccine coverage as well as manufacturers' profits. A scenario tree is used to model uncertainty in the proportions of cases from each virus strain in each stage. The authors create a branch-and-price solution algorithm and provide a heuristic to be used as a decision aid tool for the United States Food and Drug Administration.

Stochastic programming has often been studied for logistics planning during disaster responses. Barbarosoğlu and Arda (2004) propose a two-stage stochastic model for transportation planning of first-aid commodities during earthquake responses in Istanbul, Turkey. Random parameters consist of supply, arc capacity and demand. Döyen et al. (2012) propose a two-stage stochastic programming model for logistics planning in a humanitarian relief situation in which demand, warehouse capacity, and transportation time is uncertain. Decisions must be made regarding the locations of rescue centres, the amounts of inventory, the amounts distributed, and the shortage of each commodity at each location. The deterministic equivalent model is solved using a heuristic method based on Lagrangian relaxation for up to 25 scenarios. Mete and Zabinsky (2010) present a two-stage stochastic programming model for medical supply storage and distribution during disaster management. Demand amounts and transportation conditions can be affected by the disaster and are unknown. A penalty, which varies by hospital location, is included for unfulfilled demand during the second stage. This can place a priority on satisfying the demand at particular locations. Alem et al. (2016) propose a two-stage stochastic network flow model

for rapidly supplying humanitarian aid to disaster victims. The authors consider supply, demand, available financial budget, number of vehicles available for transportation, and amount of usable pre-positioned aid to be unknown.

For our problem, a two-stage stochastic programming with recourse is used to plan for PPE distribution under uncertain demand and thus we provide a review. A two-stage stochastic model with recourse is a mathematical model in which operational decisions are made during the first stage, random events occur and then new operational decisions are made in the second stage to account for the randomness that occurred between stages (Hoppe, 2007). For a general formulation, we denote $x \in \mathbb{R}^{n_1}$, $x \geq 0$ as the first-stage decision variables, where x is subject to constraints $Ax \leq b$, $A \in \mathbb{R}^{m_1 \times n_1}$, $b \in \mathbb{R}^{m_1}$. We let s be the possible scenarios that can happen during the random event and μ_s be the probability of scenario s occurring. The second-stage decision variables are $y \in \mathbb{R}^{n_2}$, $y \geq 0$, which depend on the realizations of the random events. We let $T_s \in \mathbb{R}^{m_2 \times n_1}$ and $W_s \in \mathbb{R}^{m_2 \times n_2}$ denote realizations of second-stage parameter values. The second stage is subject to the following constraints: $W_s y + T_s x = h_s$, where $h_s \in \mathbb{R}^{m_2}$. We let $c \in \mathbb{R}^{n_1}$ and $q \in \mathbb{R}^{n_2}$ be the costs associated with the first-stage and second-stage decision variables, respectively.

An example two-stage stochastic model with recourse is as follows:

$$\begin{aligned} \min \quad & c^T x + Q(x) \qquad (2.1) \\ \text{s.t.} \quad & Ax \leq b, \\ & x \geq 0, \end{aligned}$$

where

$$Q(x) := \sum_s \mu_s Q_s(x)$$

and $Q_s(x)$, the recourse function for scenario s, is given by:

$$Q_s(x) := \min\{q_s^T y \mid W_s y + T_s x = h_s\}.$$

Sample average approximation (SAA) is the main method we use to solve the two-stage stochastic program with recourse, for which we provide a review. For stochastic programs with a large number of scenarios, SAA approximates a solution by generating several independent random samples, each with fewer scenarios than the original problem. In order to approximate a solution to problem (2.1), which we will call the true problem, we define the following as the SAA problem (Verweij et al., 2003):

$$z_N = \min_x c^T x + \frac{1}{N}\sum_{s=1}^{N} Q_s(x). \tag{2.2}$$

We generate M independent samples of scenarios, each of size N. For each sample, we solve the associated SAA problem to find M objective values: $z_N^1, z_N^2, \ldots, z_N^M$ and M candidate solutions: $\hat{x}_N^1, \hat{x}_N^2, \ldots, \hat{x}_N^M$. We define $\overline{z}_N$ to be the average objective value:

$$\overline{z}_N = \frac{1}{M}\sum_{m=1}^{M} z_N^m. \tag{2.3}$$

The expected value of the average objective value is less than or equal to the optimal objective value of the true problem (Norkin et al., 1998). Thus, $\overline{z}_N$ is an estimate of the lower bound of the true problem. Given a feasible solution of the true problem, $\hat{x}$, an

estimate for the upper bound of problem (2.1) is provided by

$$\hat{z}_{N'}(\hat{x}) = c^T\hat{x} + \frac{1}{N'}\sum_{n=1}^{N'} Q_n(\hat{x}) \tag{2.4}$$

where N' is a random sample independent of the samples used to generate the feasible solution such that $N' > N$ (Verweij et al., 2003). Then, we let the estimated optimal solution of problem (2.1) be the candidate solution from the M SAA problems with the smallest estimated objective value. Thus, we set

$$\hat{x}^* = \arg\min\left\{ \hat{z}_{N'}(\hat{x}) \;\middle|\; \hat{x} \in \left\{ \hat{x}^1, \hat{x}^2, \ldots, \hat{x}^M \right\} \right\}. \tag{2.5}$$

The quality of the solution is measured using the optimality gap:

$$\hat{z}_{N'}(\hat{x}^*) - \overline{z}_N. \tag{2.6}$$

A summary of SAA is provided in Algorithm 1.

Algorithm 1: Sample Average Approximation

for *Each of the M independent samples of N scenarios* **do**

  Solve the SAA problem (2.2) using Benders decomposition;

end

Set the lower bound to be the average of all optimal objective values from the M SAA problems;

Let $\hat{x}$ be the optimal solution to the SAA problem with the smallest optimal objective value;

Create an independent random sample of size N', where $N' > N$;

Set the upper bound to be $\hat{z}_{N'}(\hat{x}) = c^T\hat{x} + \frac{1}{N'}\sum_{n=1}^{N'} Q_n(\hat{x})$;

Each SAA problem (2.2) is solved using Benders decomposition, for which we provide a review (Luedtke, 2016). Benders decomposition is an iterative solution method which begins with a small subset of the constraints and adds new constraints to the subset with each iteration. We use the assumption of relatively complete recourse, in which for every feasible first-stage solution, there exists a feasible second-stage solution. For Benders decomposition, we write the two-stage stochastic model with recourse (2.1) as follows:

$$\begin{aligned} \min \quad & c^T x + \sum_{s=1}^{S} \mu_s \theta_s \\ \text{s.t.} \quad & Ax \leq b, \\ & \theta_s \geq Q_s(x) \quad s = 1, \ldots, S \\ & x \geq 0. \end{aligned} \tag{2.7}$$

The corresponding recourse function, given $\bar{x}$, is:

$$\begin{aligned} Q_s(x) = \min_{y} \quad & q_s^T y \\ \text{s.t.} \quad & W_s y = h_s - T_s \bar{x}, \\ & y \geq 0, \end{aligned} \tag{2.8}$$

and its dual is :

$$\begin{aligned} \max_{\pi} \quad & (h_s - T_s x)^T \pi \\ \text{s.t.} \quad & W_s^T \pi \leq q. \end{aligned} \tag{2.9}$$

From problem (2.7), notice that

$$\begin{aligned}
\theta_s \geq Q_s(x) &\iff \theta_s \geq \max_{\pi} \left\{ \pi^T (h_s - T_s x) : \pi^T W_s \leq q_s \right\} \\
&\iff \theta_s \geq \max \left\{ (\pi^s)^T (h_s - T_s x) : \pi^s \in XP^s \right\} \\
&\iff \theta_s \geq (\pi^s)^T (h_s - T_s x), \pi^s \in XP^s \qquad (2.10)
\end{aligned}$$

where XP^s is the set of all extreme points of the dual (2.9) with realizations for scenario s. From (2.7) and (2.10), we get the Benders reformulation:

$$\begin{aligned}
\min \quad & c^T x + \sum_{s=1}^{S} \mu_s \theta_s \\
\text{s.t.} \quad & Ax \leq b, \\
& \theta_s \geq \pi^T (h_s - T_s x) \quad s = 1, \ldots, S; \pi^s \in XP^s \qquad (2.11) \\
& x \geq 0.
\end{aligned}$$

Constraints (2.11) are called the Benders optimality cuts. At each iteration t of Benders decomposition, a Master Problem, with a subset of the optimality cuts, is solved:

$$\begin{aligned}
z_{MP} = \quad \min \quad & c^T x + \sum_{s=1}^{S} \mu_s \theta_s \qquad (2.12) \\
\text{s.t.} \quad & Ax \leq b, \\
& \theta_s \geq (\pi^s)^T (h_s - T_s x) \quad s = 1, \ldots, S; \pi^s \in V^{s,t} \\
& x \geq 0
\end{aligned}$$

where $V^{s,t} \subseteq XP^s$. From the master problem (2.12), we obtain a solution $\left(\hat{x}^t, \hat{\theta}^t\right)$. Then

for each scenario s, solve the second-stage subproblem:

$$\begin{aligned} Q_s\left(\hat{x}^t\right) &= \min_y \left\{ q_s^T y : W_s y = h_s - T_s \hat{x}^t \right\} \\ &= \max_\pi \left\{ \pi^T \left(h_s - T_s \hat{x}^t\right) : \pi^T W_s = q_s \right\} \end{aligned}$$

and let $\hat{\pi^s}$ be the optimal dual solution. For each scenario, if the value of the second-stage recourse function is less than the optimal objective value of the subproblem (i.e. $\hat{\theta}_s^t < Q_s\left(\hat{x}^t\right)$), then add the optimal dual variable values to the subset of extreme points $V^{s,t}$ and repeat the algorithm. A lower bound is provided by the master problem objective value. An upper bound is provided by the scenario subproblems:

$$UB = c^T \hat{x}^t + \sum_{s=1}^{S} \mu_s Q_s\left(\hat{x}^t\right). \tag{2.13}$$

If the upper and lower bounds are equal, the algorithm stops and the optimal solution is found. The Benders decomposition algorithm is summarized in Algorithm 2.

If the relatively complete recourse assumption is not used, feasibility cuts need to be added for all scenarios in which the subproblem is infeasible. The feasibility cuts have the form:

$$\left(\hat{r}^s\right)^T \left(h - T_s \hat{x}^t\right) \leq 0 \tag{2.14}$$

where $\hat{r}^s$ is an extreme ray of the dual subproblem.

Scenario trees are a method of modelling uncertainty across multiple decision making stages and are often used to model scenarios in multi-stage stochastic programming. As described by Zanjani et al. (2009), scenario tree nodes represent states of the system at which new information is available to make decisions. Arcs represent events which can occur before the next stage. Each arc has an associated probability which corresponds to

the probability of using that path to arrive at the next stage. The probability of arriving at a node is the product of the probabilities of all preceding arcs on the path that led to the node. An individual scenario is represented by a path from the first stage to the last stage. All node probabilities at each stage must sum to 1.

Algorithm 2: Benders Decomposition

for *Scenario* $s = 1, 2, \ldots, S$ **do**
  Solve subproblem (2.8) correspinding to $\hat{x}^0$;
  Let $\hat{\pi}^s$ be the optimal dual solution;
  Set $V^{s,t=1} = \{\, \hat{\pi}^s \,\}$;
end
for $t = 1, 2, \ldots$ **do**
  Solve the Master Problem (2.12) with the set of constraints corresponding to $V^{s,t}$ and obtain a solution $\left(\hat{x}^t, \hat{\theta}^t\right)$;
  Set the lower bound (LB) to be the Master Problem objective value;
  for *Scenario* $s = 1, 2, \ldots, S$ **do**
    Solve the scenario subproblem for $\hat{x}^t$ and obtain $\hat{\pi}^s$ to be the optimal dual solution;
    Set $UB = c^T \hat{x}^t + \sum_{s=1}^{S} \mu_s Q_s\left(\hat{x}^t\right)$;
    if $\hat{\theta}^t < Q_s\left(\hat{x}^t\right)$ **then**
      Set $V^{s,t+1} \leftarrow V^{s,t} \cup \{\, \hat{\pi}^s \,\}$;
    end
  end
  if $LB \geq UB - \varepsilon$ **then**
    Stop;
  end
end

Chapter 3

Problem Definition

We will address the problem of PPE distribution during the COVID-19 pandemic by acquiring route and distribution centre capacity from participating carriers in order to satisfy PPE demand at the nodes (indexed by $i, j, k = 1, \ldots, J$). We assume the government controls all PPE distribution and is the entity acquiring capacity. An example network, shown in Figure 3.1, depicts two carriers, with index $r = 1, \ldots, R$, having capacity on certain routes in the network. The route capacities available from each carrier in product units are given by h_{ij}^r and the cost to acquire one product unit of capacity from carrier r for route $(i - j)$ is c_{ij}^r. It is assumed that the government will pay the same unit cost, w_{ij}, on route $i-j$ regardless of the carrier. The model could handle different costs by not using w_{ij}, and having the government pay a unit cost of c_{ij}^r along route $i-j$ for carrier r. Thus, $w_{ij} = \max_r \left\{ c_{ij}^r \right\} \ \forall i, j$. The warehouse capacities available from carrier r at location j are given by ℓ_j^r with fixed cost f_i^r. Available routes for each carrier are provided by the binary parameters u_{ij}^r, where $u_{ij}^r = 1$ indicates that carrier r serves route $i - j$. Locations with available warehouse capacity for each carrier are provided by the binary parameters v_j^r, where $v_j^r = 1$ indicates that carrier r has available storage capacity at location j. To

model the problem, the following binary decision variables are used:

$$x_{ij}^r = \begin{cases} 1, & \text{if capacity on route } (i-j) \text{ is acquired from carrier } r, \text{ and} \\ 0, & \text{otherwise,} \end{cases}$$

$$z_j^r = \begin{cases} 1, & \text{if warehouse capacity at location } j \text{ is acquired from carrier } r, \text{ and} \\ 0, & \text{otherwise.} \end{cases}$$

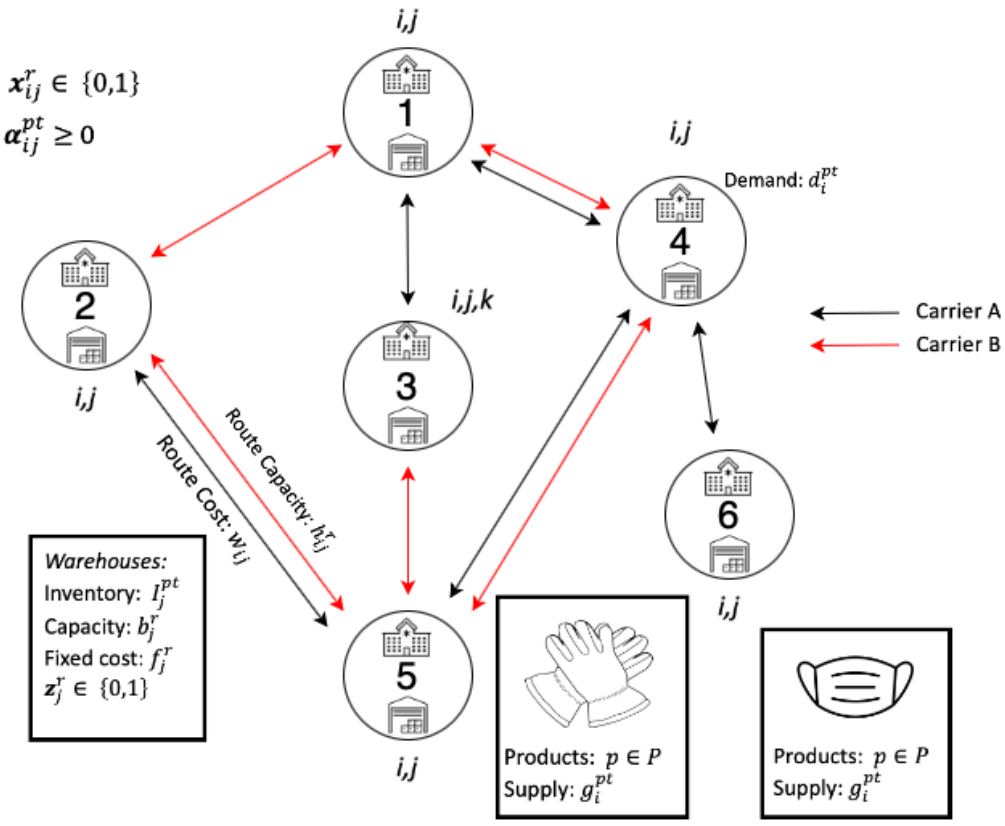

Figure 3.1: Network Diagram

PPE products, indexed by $p = 1, \ldots, P$, need to be distributed to demand nodes $i, j, k =$

$1, \ldots, J$, in time periods $t = 1, \ldots, T$, in order to satisfy demand d_i^{pt} from available supply g_i^{pt}. The amount of PPE distributed along route $(i - j)$ is represented by decision variables α_{ij}^{pt}. PPE inventory, which is represented by the decision variables I_j^{pt}, can be stored using acquired warehouse capacities. Distribution and inventory decisions are subject to maximum route capacities, h_{ij}^r, and warehouse capacities, ℓ_i^r. The parameters and decision variables are summarized in Table 3.1. Under sufficient supply, the capacity acquisition and PPE distribution model is:

$$[DET]:$$

$$\min \quad \sum_i \sum_j \sum_r w_{ij} h_{ij}^r x_{ij}^r + \sum_j \sum_r f_j^r z_j^r \tag{3.1}$$

$$\text{s.t.} \quad x_{ij}^r \leq u_{ij}^r \qquad i, j = 1, \ldots, J; r = 1, \ldots, R \tag{3.2}$$

$$z_j^r \leq v_j^r \qquad j = 1, \ldots, J; r = 1, \ldots, R \tag{3.3}$$

$$\sum_p \alpha_{ij}^{pt} \leq \sum_r h_{ij}^r x_{ij}^r \qquad i, j = 1, \ldots, J; r = 1, \ldots, R \tag{3.4}$$

$$\sum_i \alpha_{ij}^{pt} + I_j^{p(t-1)} + g_j^{pt} = d_j^{pt} + \sum_k \alpha_{jk}^{pt} + I_j^{pt}$$
$$j = 1, \ldots, J; p = 1, \ldots, P; t = 2, \ldots, T \tag{3.5}$$

$$\sum_i \alpha_{ij}^{pt} + g_j^{pt} = d_j^{pt} + \sum_k \alpha_{jk}^{pt} + I_j^{pt}$$
$$j = 1, \ldots, J; p = 1, \ldots, P; t = 1 \tag{3.6}$$

$$\sum_p I_j^{pt} \leq \sum_r \ell_j^r z_j^r \qquad j = 1, \ldots, J; t = 1, \ldots, T \tag{3.7}$$

$$x_{ij}^r, z_j^r \in \{0, 1\} \qquad i, j = 1, \ldots, J; r = 1, \ldots, R \tag{3.8}$$

$$\alpha_{ij}^{pt}, I_j^{pt} \geq 0 \qquad i, j = 1, \ldots, J; p = 1, \ldots, P; t = 1, \ldots, T. \tag{3.9}$$

The objective function (3.1) minimizes the total cost of satisfying all demand within the network. The first term of the objective function represents the of acquiring route capacity from carriers. The product $w_{ij}h_{ij}^r$ denotes the cost of transporting the required PPE from location i to location j using carrier r. The binary decision variable x_{ij}^r represents whether route capacity as been acquired. The second term of the objective function represents the cost of acquiring warehouse capacity in the network. Constraints (3.2) ensure that route capacity cannot be acquired from a carrier unless the carrier has capacity along the route. Constraints (3.3) ensure that storage capacity at a location cannot be acquired from a carrier unless the carrier has warehouse capacity available at that location. Constraints (3.2) and (3.3) are included for completeness, however these constraints are not needed in implementation as x_{ij} variables corresponding to $u_{ij}^r = 0$ and $v_j^r = 0$ are simply removed. Constraints (3.4) ensure that products cannot be distributed along a route unless capacity along the route has been acquired and that the amount of product distributed on a route does not exceed the acquired capacity for each carrier. If route capacity is acquired on a particular route, then $x_{ij}^r = 1$ and the amount of product distributed on that route must not exceed the available capacity. If route capacity is not acquired on a route, then $x_{ij}^r = 0$ and no product can be distributed on that route. Constraints (3.5) and (3.6) ensure that incoming PPE is equivalent to the outgoing PPE at each node for each time period. Incoming PPE consists of incoming distribution, previous inventory and supply. Outgoing PPE consists of demand, outgoing distribution, and current inventory. Constraints (3.6) consider only the first time period and specify that nodes do not start with any inventory, while Constraints (3.5) consider all remaining time periods. Thus for the first time period, incoming PPE at a location consists only of incoming distribution and supply at the location. Constraints (3.7) ensure that inventory cannot be stored at a node

unless warehouse capacity has been acquired and that the inventory does not exceed the capacity at the warehouse. If distribution centre capacity has been acquired at a particular location, then $z_j^r = 1$ and the amount of inventory stored at the location must not exceed the available capacity. If distribution centre capacity has not been acquired at a location, then $z_j^r = 0$ and no PPE can be stored as inventory at the location. Constraints (3.8) ensure that x_{ij}^r and z_j^r decision variables are binary and Constraints (3.9) specify that the α_{ij}^{pt} and I_j^{pt} decision variables are continuous and non-negative.

The following sections extend the previous models under different settings. Section 3.1 considers the PPE supply shortage case where PPE distribution must be prioritized. Section 3.2 considers the uncertain demand case due to varying COVID-19 risk levels.

3.1 Insufficient Supply

The problem can be extended to consider a situation in which there is insufficient supply to satisfy demand at all nodes in the network. In this case, the available PPE must be distributed among the nodes in an equitable way to prevent some nodes from receiving their full demand while other nodes receive no demand. The amount of PPE a location receives should reflect demand as well as the severity of the COVID-19 pandemic at the location. For example, a node with a lot of COVID-19 cases should require more PPE than a node with fewer cases.

To model this problem extension, nodes are assigned priorities (q_i) which reflect their need for PPE. A term is added to the objective function which emphasizes distribution to locations with high demand and high priority. The variable ρ_j^{pt} represents the proportion of the demand for product p received at location j during time period t. The scalar τ is a

Table 3.1: Summary of Notation

Indices	
i, j, k	network nodes
r	carriers
p	products
t	times
s	scenarios
Parameters	
g_i^{tp}	supply of product p from node i at time t
d_i^{tp}	demand for product p at node i at time t
ℓ_i^r	capacity of warehouse for carrier r at node i
c_{ij}^r	cost that carrier r charges for one product unit of capacity on route $(i-j)$
w_{ij}	cost the government pays to acquire on product unit of capacity on route $(i-j)$
f_i^r	fixed cost to acquire warehouse capacity from carrier r at node i
h_{ij}^r	route capacity per product unit per time period for carrier r along route $(i-j)$
u_{ij}^r	$= 1$ if carrier r has route capacity available along route $(i-j)$; and 0 otherwise
v_i^r	$= 1$ if carrier r has warehouse capacity available at node i; and 0 otherwise
q_i	priority of destination city i
μ_s	probability of second-stage scenario s occurring
d_k^{pts}	demand for product p of node k for time period t during scenario s
γ_{ij}	unit cost of increasing distribution on route $(i-j)$ during the second stage
φ_{ij}	unit cost recovered from decreasing distribution along route $(i-j)$ during the second stage
Decision Variables	
x_{ij}^r	$= 1$ if capacity is acquired on route $(i-j)$ from carrier r; and 0 otherwise
z_i^r	$= 1$ if warehouse capacity is acquired from carrier r at location i; and 0 otherwise
α_{ij}^{tp}	amount of product p being shipped on route $(i-j)$ for time period t as decided during the first stage
I_i^{pt}	inventory of product p stored at node i at time period t
m_{ij}^{pts}	the increase in distribution of product p on route $(i-j)$ in time period t for scenario s
n_{ij}^{pts}	the decrease in distribution of product p on route $(i-j)$ in time period t for scenario s
I_i^{pts}	the amount of inventory stored at location i for product p for time period t for scenario s

weight parameter which ensures that the third term is large enough to impact the objective function. The priority model for insufficient supply is as follows:

$$[PRI]:$$

$$\min \quad \sum_i \sum_j \sum_r w_{ij} h_{ij}^r x_{ij}^r + \sum_j \sum_r f_j^r z_j^r + \sum_j \sum_p \sum_t \frac{\tau}{q_j \rho_j^{pt} d_j^{pt}} \tag{3.10}$$

$$\text{s.t.} \quad x_{ij}^r \le u_{ij}^r \qquad i,j = 1,\ldots,J; p = r,\ldots,R \tag{3.11}$$

$$z_j^r \le v_j^r \qquad j = 1,\ldots,J; r = 1,\ldots,R \tag{3.12}$$

$$\sum_p \alpha_{ij}^{pt} \le \sum_r h_{ij}^r x_{ij}^r \qquad i,j = 1,\ldots,J; r = 1,\ldots,R \tag{3.13}$$

$$\sum_i \alpha_{ij}^{pt} + I_j^{p(t-1)} + g_j^{pt} = \rho_j^{pt} d_j^{pt} + \sum_k \alpha_{jk}^{pt} + I_j^{pt}$$
$$j = 1,\ldots,J; p = 1,\ldots,P; t = 2,\ldots,T \tag{3.14}$$

$$\sum_i \alpha_{ij}^{pt} + g_j^{pt} = \rho_j^{pt} d_j^{pt} + \sum_k \alpha_{jk}^{pt} + I_j^{pt}$$
$$j = 1,\ldots,J; p = 1,\ldots,P; t = 1 \tag{3.15}$$

$$\sum_p I_j^{pt} \le \sum_r \ell_j^r z_j^r \qquad j = 1,\ldots,J; t = 1,\ldots,T \tag{3.16}$$

$$\rho_j^{pt} \le 1 \qquad j = 1\ldots,J; p = 1,\ldots,P; t = 1,\ldots,T \tag{3.17}$$

$$x_{ij}^r, z_j^r \in \{0,1\} \qquad i,j = 1,\ldots,J; r = 1,\ldots,R \tag{3.18}$$

$$\alpha_{ij}^{pt}, I_j^{pt}, \rho_j^{pt} \ge 0 \qquad i,j = 1,\ldots,J; p = 1,\ldots,P; t = 1,\ldots,T. \tag{3.19}$$

The objective function (3.10) minimizes the total cost of acquiring route and warehouse capacity and maximizes the proportion of each location's demand received. The value of the third term will decrease as a higher proportion of demand is received. The decrease

will be larger for nodes with large demand and high priority values, thus encouraging the distribution of PPE to such nodes. In order to be solved by optimization software, such as Gurobi, the model is reformulated as follows:

$[PRI2]$:

$$\min \quad \sum_i \sum_j \sum_r w_{ij} h_{ij}^r x_{ij}^r + \sum_j \sum_r f_j^r z_j^r + \sum_j \sum_p \sum_t \frac{\tau}{q_j d_j^{pt}} Y_j^{pt} \tag{3.20}$$

$$\text{s.t.} \quad x_{ij}^r \leq u_{ij}^r \qquad i,j = 1,\ldots,J; r = 1,\ldots,R \tag{3.21}$$

$$z_j^r \leq v_j^r \qquad j = 1,\ldots,J; r = 1,\ldots,R \tag{3.22}$$

$$\sum_p \alpha_{ij}^{pt} \leq \sum_r h_{ij}^r x_{ij}^r \qquad i,j = 1,\ldots,J; r = 1,\ldots,R \tag{3.23}$$

$$\sum_i \alpha_{ij}^{pt} + I_j^{p(t-1)} + g_j^{pt} = \rho_j^{pt} d_j^{pt} + \sum_k \alpha_{jk}^{pt} + I_j^{pt}$$
$$j = 1,\ldots,J; p = 1,\ldots,P; t = 1,\ldots,T \tag{3.24}$$

$$\sum_i \alpha_{ij}^{pt} + g_j^{pt} = \rho_j^{pt} d_j^{pt} + \sum_k \alpha_{jk}^{pt} + I_j^{pt}$$
$$j = 1,\ldots,J; p = 1,\ldots,P; t = 0 \tag{3.25}$$

$$\sum_p I_j^{pt} \leq \sum_r \ell_j^r z_j^r \qquad j = 1,\ldots,J; t = 1,\ldots,T \tag{3.26}$$

$$\rho_j^{pt} \leq 1 \qquad j = 1\ldots,J; p = 1,\ldots,P; t = 1,\ldots,T \tag{3.27}$$

$$Y_j^{pt} \rho_j^{pt} \geq 1 \qquad j = 1,\ldots,J; p = 1\ldots,P; t = 1\ldots,T \tag{3.28}$$

$$x_{ij}^r, z_j^r \in \{0,1\} \qquad i,j = 1,\ldots,J; r = 1,\ldots,R \tag{3.29}$$

$$\alpha_{ij}^{pt}, I_j^{pt}, \rho_j^{pt} \geq 0 \qquad i,j = 1,\ldots,J; p = 1,\ldots,P; t = 1,\ldots,T. \tag{3.30}$$

The variable Y_j^{pt} is added in place of $\frac{1}{\rho_j^{pt}}$ and Constraints (3.28) are added to restrict Y_j^{pt}.

By including the new variable in the objective function, the objective function becomes linear. Even though Constraints (3.28) are non-linear, $[PRI2]$ is a second-order cone program, which can be solved directly with optimization software.

3.2 Pandemic Uncertainty

The problem can also be extended to incorporate uncertain demand. This uncertainty is due to unknown future COVID-19 risk levels at different locations. As the severity of the COVID-19 pandemic increases, more PPE is required for healthcare workers and for the population to combat the virus. This extension is modelled as a two-stage stochastic model with recourse. Decisions for route and warehouse capacity acquisitions as well as for initial distribution are made in the first stage. Then, once a scenario s with known demand d_k^{pts} is realized, the distribution decisions can be modified in the second stage. Each scenario is realized with probability μ_s. Second stage decision variables consist of increases and decreases to the amount of PPE being distributed and of inventory quantities, which are represented by m_{ij}^{pts}, n_{jk}^{pts}, and I_i^{pts}, respectively.

The variables m_{ijs}^{pt} and n_{jks}^{pt} allow for PPE rerouting. Depending on the scenario realization, PPE may have to be added or removed from a route in order to accomodate for the changes in demand. Should a unit of demand be added to the route during the second stage, the unit transportation cost is γ_{ij}. Should a unit of demand be removed from the route during the second stage, the unit cost recovered is φ_{ij}. It is assumed that $\gamma_{ij} \geq w_{ij} \ \forall i, j$ and $\phi_{ij} \leq w_{ij} \ \forall i, j$. These assumptions imply that the cost to distribute product is greater if the decision is made last-minute as opposed to in advance and that not all costs will be recovered if a removal decision is made last-minute. The two-stage stochastic model with recourse is as follows:

$[STOCH]$:

$$\min \quad \sum_i \sum_j \sum_r w_{ij} h_{ij}^r x_{ij}^r + \sum_j \sum_r f_j^r z_j^r + \sum_s \mu_s Q_s \left(x_{ij}^r, z_j^r, \alpha_{ij}^{pt} \right) \tag{3.31}$$

s.t.
$$x_{ij}^r \leq u_{ij}^r \qquad i,j = 1,\ldots,J; r = 1,\ldots,R \tag{3.32}$$

$$z_j^r \leq v_j^r \qquad j = 1,\ldots,J; r = 1,\ldots,R \tag{3.33}$$

$$\sum_p \alpha_{ij}^{pt} \leq \sum_r h_{ij}^r x_{ij}^r \qquad i,j = 1,\ldots,J; t = 1,\ldots,T \tag{3.34}$$

$$\sum_i \alpha_{ij}^{pt} + I_j^{p(t-1)} + g_j^{pt} = d_j^{pt} + \sum_k \alpha_{jk}^{pt} + I_j^{pt}$$
$$j = 1,\ldots,J; p = 1,\ldots,P; t = 2,\ldots,T \tag{3.35}$$

$$\sum_i \alpha_{ij}^{pt} + g_j^{pt} = d_j^{pt} + \sum_k \alpha_{jk}^{pt} + I_j^{pt}$$
$$j = 1,\ldots,J; p = 1,\ldots,P; t = 1 \tag{3.36}$$

$$\sum_p I_j^{pt} \leq \sum_r \ell_j^r z_j^r \qquad j = 1,\ldots,J; t = 1,\ldots,T \tag{3.37}$$

$$x_{ij}^r, z_j^r \in \{0,1\} \qquad i,j = 1,\ldots,J; r = 1,\ldots,R \tag{3.38}$$

$$\alpha_{ij}^{pt}, I_j^{pt} \geq 0 \qquad i,j = 1,\ldots,J; p = 1,\ldots,P; t = 1,\ldots,T \tag{3.39}$$

where

$$Q_s\left(x_{ij}^r, z_j^r, \alpha_{ij}^{pt}\right) = \min \sum_i \sum_j \sum_p \sum_t \left(\gamma_{ij} m_{ij}^{pts} - \varphi_{ij} n_{ij}^{pts}\right) \tag{3.40}$$

$$\text{s.t.} \quad \sum_p \left(\alpha_{ij}^{pt} + m_{ij}^{pts} - n_{ij}^{pts}\right) \leq \sum_r h_{ij}^r x_{ij}^r$$
$$i, j = 1, \ldots, J; t = 1, \ldots, T \tag{3.41}$$

$$\sum_i \left(\alpha_{ij}^{pt} + m_{ij}^{pts} - n_{ij}^{pts}\right) + I_{js}^{p(t-1)s} + g_j^{pt}$$
$$= d_j^{pts} + \sum_k \left(\alpha_{jk}^{pt} + m_{jk}^{pts} - n_{jk}^{pts}\right) + I_j^{pts}$$
$$j = 1, \ldots, J; p = 1, \ldots, P; t = 2, \ldots, T \tag{3.42}$$

$$\sum_i \left(\alpha_{ij}^{pt} + m_{ij}^{pts} - n_{ij}^{pts}\right) + g_j^{pt}$$
$$= d_j^{pts} + \sum_k \left(\alpha_{jk}^{pt} + m_{jk}^{pts} - n_{jk}^{pts}\right) + I_j^{pts}$$
$$j = 1, \ldots, J; p = 1, \ldots, P; t = 1 \tag{3.43}$$

$$\sum_p I_j^{pts} \leq \sum_r \ell_j^r z_j^r \qquad j = 1, \ldots, J; t = 1, \ldots, T \tag{3.44}$$

$$n_{ij}^{pts} \leq \alpha_{ij}^{pt} \quad i, j = 1, \ldots, J; p = 1, \ldots, P; t = 1, \ldots, T \tag{3.45}$$

$$m_{ij}^{pts}, n_{ij}^{pts}, I_i^{pts} \geq 0 \;\; i, j = 1, \ldots, J; p = 1, \ldots, P;$$
$$t = 1, \ldots, T; s = 1, \ldots, S. \tag{3.46}$$

The objective function (3.31) minimizes the total cost of acquiring route and warehouse capacity as well as the expected cost of rerouting the PPE distribution for all scenarios during the second stage, $Q_s\left(x_{ij}^r, z_j^r, \alpha_{ij}^{pt}\right)$. The second-stage objective (3.40) minimizes the

cost of changing the distribution for a scenario s. Constraints (3.41) and ensure that product cannot be distributed unless route capacity has been acquired and that the amount of product distributed does not exceed the route capacity. The amount of product distributed consists of the first-stage amount (α_{ij}^{pt}), the second-stage increase (m_{ij}^{pts}) and the second-stage decrease (n_{ij}^{pts}). Constraints (3.42) ensure that the incoming PPE is equivalent to the outgoing PPE at each node for each time period after second-stage changes. Incoming PPE consists of incoming distribution, previous inventory and supply. Outgoing PPE consists of node demand, outgoing distribution, and current inventory. Constraints (3.43) explicitly say that nodes cannot start with any inventory. Constraints (3.44) ensure that the amounts of PPE stored as inventory after the second-stage changes do not exceed the acquired storage capacity. Constraints (3.45) ensure that we do not remove more PPE of each type than we initially assigned to each route during each time period. Constraints (3.46) ensure that the second-stage decision variables are continuous and non-negative.

In the following section, we derive a Benders decomposition approach to solve the two-stage stochastic program with recourse.

3.2.1 Benders Decomposition

For fixed first-stage decisions, namely the capacity acquired $\left(\bar{x}_{ij}^{r}, \bar{z}_{j}^{r}\right)$ and the initial distribution and inventory allocation $\bar{\alpha}_{ij}^{pt}$ and $\bar{I}_{j}^{pt}$, the second stage decisions are:

$$[SP(s)]: \quad Q_s\left(\bar{x}_{ij}^r, \bar{z}_j^r, \bar{\alpha}_{ij}^{pt}\right) =$$

$$\min \quad \sum_i \sum_j \sum_p \sum_t \left(\gamma_{ij} m_{ij}^{pts} - \varphi_{ij} n_{ij}^{pts}\right) \tag{3.47}$$

$$\text{s.t.} \quad \sum_p \left(m_{ij}^{pts} - n_{ij}^{pts}\right) \leq \sum_r h_{ij}^r \bar{x}_{ij}^r - \sum_p \bar{\alpha}_{ij}^{pt}$$

$$i, j = 1, \ldots, J; t = 1, \ldots, T \qquad \longrightarrow \pi_{ij}^{1ts} \tag{3.48}$$

$$\sum_i \left(m_{ij}^{pts} - n_{ij}^{pts}\right) - \sum_k \left(m_{jk}^{pts} - n_{jk}^{pts}\right) + I_j^{p(t-1)s} - I_j^{pts}$$

$$= d_j^{pts} - g_j^{pt} + \sum_k \bar{\alpha}_{jk}^{pt} - \sum_i \bar{\alpha}_{ij}^{pt}$$

$$j = 1, \ldots, J; p = 1, \ldots, P; t = 2, \ldots, T \quad \longrightarrow \pi_j^{2pts} \tag{3.49}$$

$$\sum_i \left(m_{ij}^{pts} - n_{ij}^{pts}\right) - \sum_k \left(m_{jk}^{pts} - n_{jk}^{pts}\right) - I_j^{pts}$$

$$= d_j^{pts} - g_j^{pt} + \sum_k \bar{\alpha}_{jk}^{pt} - \sum_i \bar{\alpha}_{ij}^{pt}$$

$$j = 1, \ldots, J; p = 1, \ldots, P; t = 1 \qquad \longrightarrow \pi_j^{3ps} \tag{3.50}$$

$$\sum_p I_{js}^{pt} \leq \sum_r \ell_j^r \bar{z}_j^r \qquad j = 1, \ldots, J; t = 1, \ldots, T \qquad \longrightarrow \pi_j^{4ts} \tag{3.51}$$

$$n_{ij}^{pts} \leq \bar{\alpha}_{ij}^{pt} \quad i, j = 1, \ldots, J; p = 1, \ldots, P, t = 1, \ldots, T \longrightarrow \pi_{ij}^{5pts} \tag{3.52}$$

$$m_{ij}^{pts}, n_{ij}^{pts}, I_i^{pts} \geq 0 \quad i, j = 1, \ldots, J; p = 1, \ldots, P;$$

$$t = 1, \ldots, T; s = 1, \ldots, S. \tag{3.53}$$

This is referred to as the Benders primal subproblem. We note that it is not decom-

posable by time period t due to Constraints (3.49) and (3.50). The dual of $[SP(s)]$ is:

$[DSP(s)]$:

$$\begin{aligned}
\max \quad & \sum_i \sum_j \sum_t \left(\sum_r h_{ij}^r \bar{x}_{ij}^r - \sum_p \bar{\alpha}_{ij}^{pt} \right) \pi_{ij}^{1ts} \\
& + \sum_j \sum_p \sum_t \left(d_{js}^{pt} - g_j^{pt} + \sum_k \bar{\alpha}_{jk}^{pt} - \sum_i \bar{\alpha}_{ij}^{pt} \right) \pi_j^{2pts} \\
& + \sum_j \sum_p \left(d_{js}^{p,t=1} - g_j^{p,t=1} + \sum_k \bar{\alpha}_{jk}^{p,t=1} - \sum_i \bar{\alpha}_{ij}^{p,t=1} \right) \pi_j^{3ps} \\
& + \sum_j \sum_t \sum_r \left(\ell_j^r \bar{z}_j^r \right) \pi_j^{4ts} + \sum_i \sum_j \sum_p \sum_t \bar{\alpha}_{ij}^{pt} \pi_{ij}^{5pts} \qquad (3.54) \\
\text{s.t.} \quad & \pi \in FS^{\pi} \qquad (3.55)
\end{aligned}$$

where $\pi = \left(\pi_{ij}^{1ts}, \pi_j^{2pts}, \pi_j^{3ps}, \pi_j^{4ts}, \pi_{ij}^{5pts}\right)$ are the dual variables corresponding to Constraints (3.48) - (3.52) and FS^{π} is the feasible set of $[DSP(s)]$ that is not written explicitly for ease of exposition.

The combined first-stage and $[SP(s)]$ solutions provide a feasible solution and an upper bound on the optimal objective of $[STOCH]$. Benders cuts based on $[DSP(s)]$ are added to the following master problem:

$[BMP]$:

$$\begin{aligned}
\min \quad & \sum_i \sum_j \sum_r w_{ij} h_{ij}^r x_{ij}^r + \sum_j \sum_r f_j^r z_j^r + \sum_s \mu_s \theta_s \qquad (3.56) \\
\text{s.t.} \quad & x_{ij}^r \leq u_{ij}^r \qquad i, j = 1, \ldots, J; r = 1, \ldots, R \qquad (3.57) \\
& z_j^r \leq v_j^r \qquad j = 1, \ldots, J; r = 1, \ldots, R \qquad (3.58)
\end{aligned}$$

$$\sum_p \alpha_{ij}^{pt} \leq \sum_r h_{ij}^r x_{ij}^r \qquad i,j = 1,\ldots,J; t = 1,\ldots,T \tag{3.59}$$

$$\sum_i \alpha_{ij}^{pt} + I_j^{p(t-1)} + g_j^{pt} = d_j^{pt} + \sum_k \alpha_{jk}^{pt} + I_j^{pt}$$
$$j = 1,\ldots,J; p = 1,\ldots,P; t = 2,\ldots,T \tag{3.60}$$

$$\sum_i \alpha_{ij}^{pt} + g_j^{pt} = d_j^{pt} + \sum_k \alpha_{jk}^{pt} + I_j^{pt}$$
$$j = 1,\ldots,J; p = 1,\ldots,P; t = 1 \tag{3.61}$$

$$\sum_p I_j^{pt} \leq \sum_r \ell_j^r z_j^r \qquad j = 1,\ldots,J; t = 1,\ldots,T \tag{3.62}$$

$$\begin{aligned}\theta_s^b \geq & \sum_i \sum_j \sum_t \left(\sum_r h_{ij}^r x_{ij}^r - \sum_p \alpha_{ij}^{pt} \right) \pi_{ij}^{1tsb} \\ & + \sum_j \sum_p \sum_t \left(d_j^{pts} - g_j^{pt} + \sum_k \alpha_{jk}^{pt} - \sum_i \alpha_{ij}^{pt} \right) \pi_j^{2ptsb} \\ & + \sum_j \sum_p \left(d_j^{p,t=1,s} - g_j^{p,t=1} + \sum_k \alpha_{jk}^{p,t=1} - \sum_i \alpha_{ij}^{p,t=1} \right) \pi_j^{3psb} \\ & + \sum_j \sum_t \sum_r \left(\ell_j^r z_j^r \right) \pi_j^{4tsb} + \sum_i \sum_j \sum_p \sum_t \alpha_{ij}^{pt} \pi_{ij}^{5ptsb} \\ & b \in B^s; s = 1,\ldots,S \end{aligned} \tag{3.63}$$

$$\begin{aligned} 0 \geq & \sum_i \sum_j \sum_t \left(\sum_r h_{ij}^r x_{ij}^r - \sum_p \alpha_{ij}^{pt} \right) \pi_{ij}^{1tsb} \\ & + \sum_j \sum_p \sum_t \left(d_j^{pts} - g_j^{pt} + \sum_k \alpha_{jk}^{pt} - \sum_i \alpha_{ij}^{pt} \right) \pi_j^{2ptsb} \\ & + \sum_j \sum_p \left(d_j^{p,t=1,s} - g_j^{p,t=1} + \sum_k \alpha_{jk}^{p,t=1} - \sum_i \alpha_{ij}^{p,t=1} \right) \pi_j^{3psb} \\ & + \sum_j \sum_t \sum_r \left(\ell_j^r z_j^r \right) \pi_j^{4tsb} + \sum_i \sum_j \sum_p \sum_t \alpha_{ij}^{pt} \pi_{ij}^{5ptsb} \\ & b \in E^s; s = 1,\ldots,S \end{aligned} \tag{3.64}$$

$$x_{ij}^r, z_j^r \in \{0,1\} \qquad i,j = 1,\ldots,J; r = 1,\ldots,R \tag{3.65}$$

$$\alpha_{ij}^{pt} \geq 0 \qquad i,j = 1,\ldots,J; p = 1,\ldots,P; t = 1,\ldots,T. \tag{3.66}$$

For the Benders master problem, we begin with the first-stage problem from $[STOCH]$ and we add the sets of constraints (3.63) and (3.64). Constraints (3.63) are the optimality cuts, where B^s is the set of extreme point dual solutions of FS^π for scenario s. Constraints (3.64) are the feasibility cuts where E^s is the set of extreme rays of the dual feasible region of FS^π for scenario s.

For iteration $\mathcal{T}$ of the Benders decomposition algorithm, the upper bound is:

$$UB^{\mathcal{T}} = \sum_i \sum_j \sum_r w_{ij} h_{ij}^r \bar{x}_{ij}^r + \sum_j \sum_r f_j^r \bar{z}_j^r + \sum_s \mu_s \sum_i \sum_j \sum_p \sum_t \left(\gamma_{ij} \bar{m}_{ij}^{pts} - \varphi_{ij} \bar{n}_{ij}^{pts}\right)$$

where $\bar{x}_{ij}^r$ and $\bar{z}_j^r$ are the Benders Master Problem solution and $\bar{m}_{ij}^{pts}$ and $\bar{n}_{ij}^{pts}$ are the solutions to the subproblems. The best upper bound is provided by $UB = \min\left\{ UB, UB^{\mathcal{T}} \right\}$. The lower bound is the objective of the relaxed master problem $[BMP]$ at iteration $\mathcal{T}$.

3.2.2 Sample Average Approximation

Two-stage stochastic models with recourse can be approximated using sample average approximation. The true problem $[STOCH]$ can be approximated by solving the SAA problem M times. Each SAA problem will be solved with an independent random sample

of scenarios of size N. The SAA problem for each of the M samples is:

$[SAA]$:

$$\mathcal{Z}_n^M = \min \quad \sum_i \sum_j \sum_r w_{ij} h_{ij}^r x_{ij}^r + \sum_j \sum_r f_j^r z_j^r + \frac{1}{N} \sum_{n=1}^{N} Q_n \left(x_{ij}^r, z_j^r, \alpha_{ij}^{pt} \right)$$

$$\text{s.t.} \quad x_{ij}^r \leq u_{ij}^r \qquad i,j = 1,\ldots,J; r = 1,\ldots,R \tag{3.67}$$

$$z_j^r \leq v_j^r \qquad j = 1,\ldots,J; r = 1,\ldots,R \tag{3.68}$$

$$\sum_p \alpha_{ij}^{pt} \leq \sum_r h_{ij}^r x_{ij}^r \qquad i,j = 1,\ldots,J; t = 1,\ldots,T \tag{3.69}$$

$$\sum_i \alpha_{ij}^{pt} + I_j^{p(t-1)} + g_j^{pt} = d_j^{pt} + \sum_k \alpha_{jk}^{pt} + I_j^{pt}$$
$$j = 1,\ldots,J; p = 1,\ldots,P; t = 2,\ldots,T \tag{3.70}$$

$$\sum_i \alpha_{ij}^{pt} + g_j^{pt} = d_j^{pt} + \sum_k \alpha_{jk}^{pt} + I_j^{pt}$$
$$j = 1,\ldots,J; p = 1,\ldots,P; t = 1 \tag{3.71}$$

$$\sum_p I_j^{pt} \leq \sum_r \ell_j^r z_j^r \qquad j = 1,\ldots,J; t = 1,\ldots,T \tag{3.72}$$

$$x_{ij}^r, z_j^r \in \{0,1\} \qquad i,j = 1,\ldots,J; r = 1,\ldots,R \tag{3.73}$$

$$\alpha_{ij}^{pt}, I_j^{pt} \geq 0 \qquad i,j = 1,\ldots,J; p = 1,\ldots,P; t = 1,\ldots,T. \tag{3.74}$$

An estimate of the lower bound is given by:

$$\overline{\mathcal{Z}}_N = \frac{1}{M} \sum_{m=1}^{M} z_n^M. \tag{3.75}$$

.

For a given feasible first-stage solution $\left(\bar{x}_{ij}^{r}, \bar{z}_{ij}^{r}, \bar{\alpha}_{ij}^{pt}\right)$, an estimate of the upper bound is given by:

$$\bar{\mathcal{Z}}_{N'}\left(\bar{x}_{ij}^{r}, \bar{z}_{ij}^{r}, \bar{\alpha}_{ij}^{pt}\right) = \sum_{i}\sum_{j}\sum_{r} w_{ij} h_{ij}^{r} \bar{x}_{ij}^{r} + \sum_{j}\sum_{r} f_{j}^{r} \bar{z}_{j}^{r} + \frac{1}{N'}\sum_{n=1}^{N'} Q_{n}\left(\bar{x}_{ij}^{r}, \bar{z}_{j}^{r}, \bar{\alpha}_{ij}^{pt}\right). \quad (3.76)$$

Chapter 4 describes the data used to test the above models. In Chapter 5, we provide numerical testing.

Chapter 4

Data

The proposed framework will be applied to the province of Ontario, where the nodes are the provincial health regions. The Ontario health regions are given in Figures 4.1 and 4.2. We consider two types of PPE: surgical masks and surgical gowns and a single box of either type of PPE is considered to have the same dimensions. Thus, a box of 50 surgical masks and a box of 20 surgical gowns are each considered to be one unit.

Demand for each health region was calculated based on the number of healthcare workers in each region according to the 2016 Census (Statistics Canada, 2020). The census data includes people in all health occupations such as physicians, nurses, technicians, optometrists, dentists, etc. It is assumed that healthcare workers use four masks and four gowns per day. Weekly demand for a health region, in number of boxes of PPE, was calculated as follows:

$$\begin{aligned} &\textit{Weekly demand} \\ &= \frac{(\#\ \textit{of healthcare workers})\,(\textit{PPE usage per person per day})\,(5\ \textit{work days per week})}{(\#\ \textit{of items per box})}. \end{aligned}$$

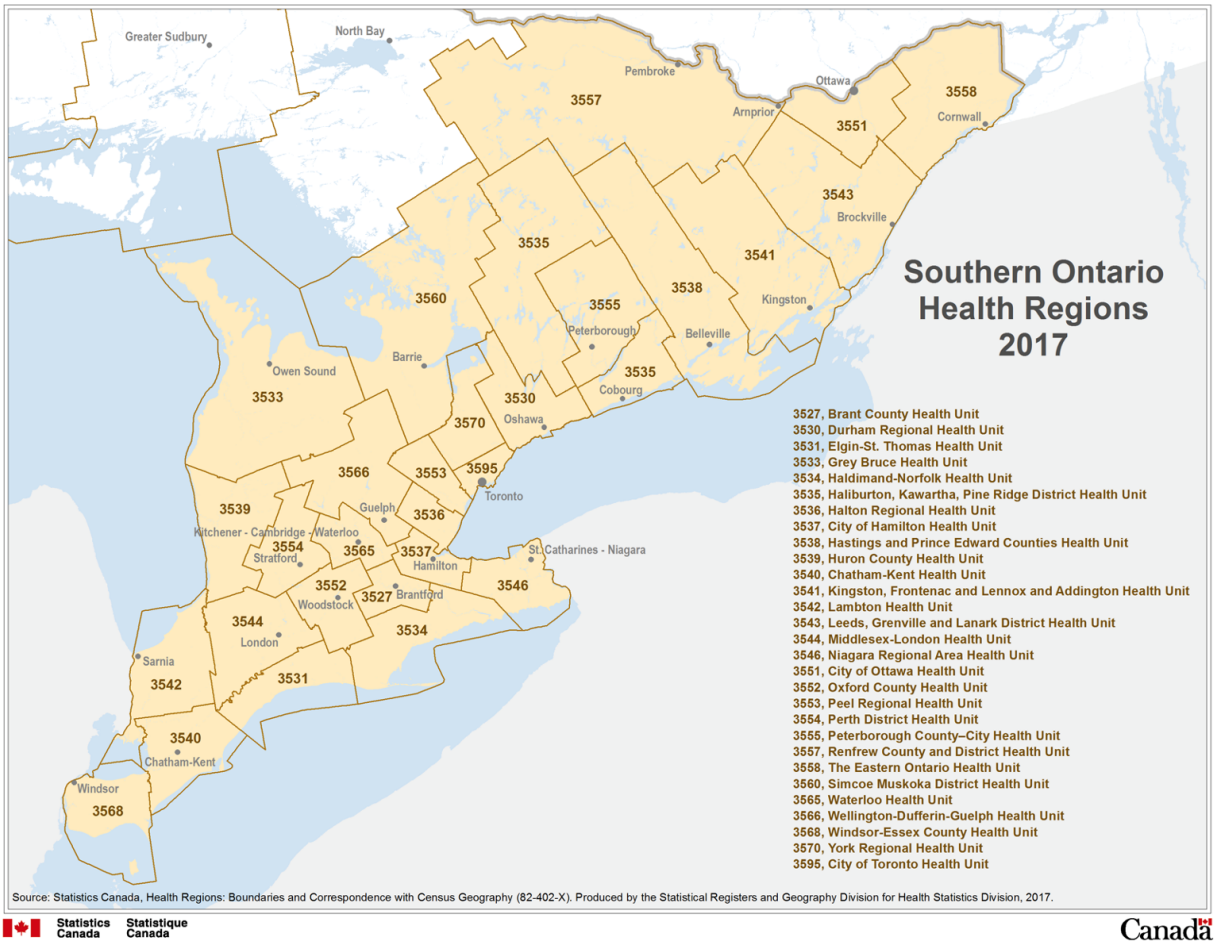

Figure 4.1: Southern Ontario Health Regions

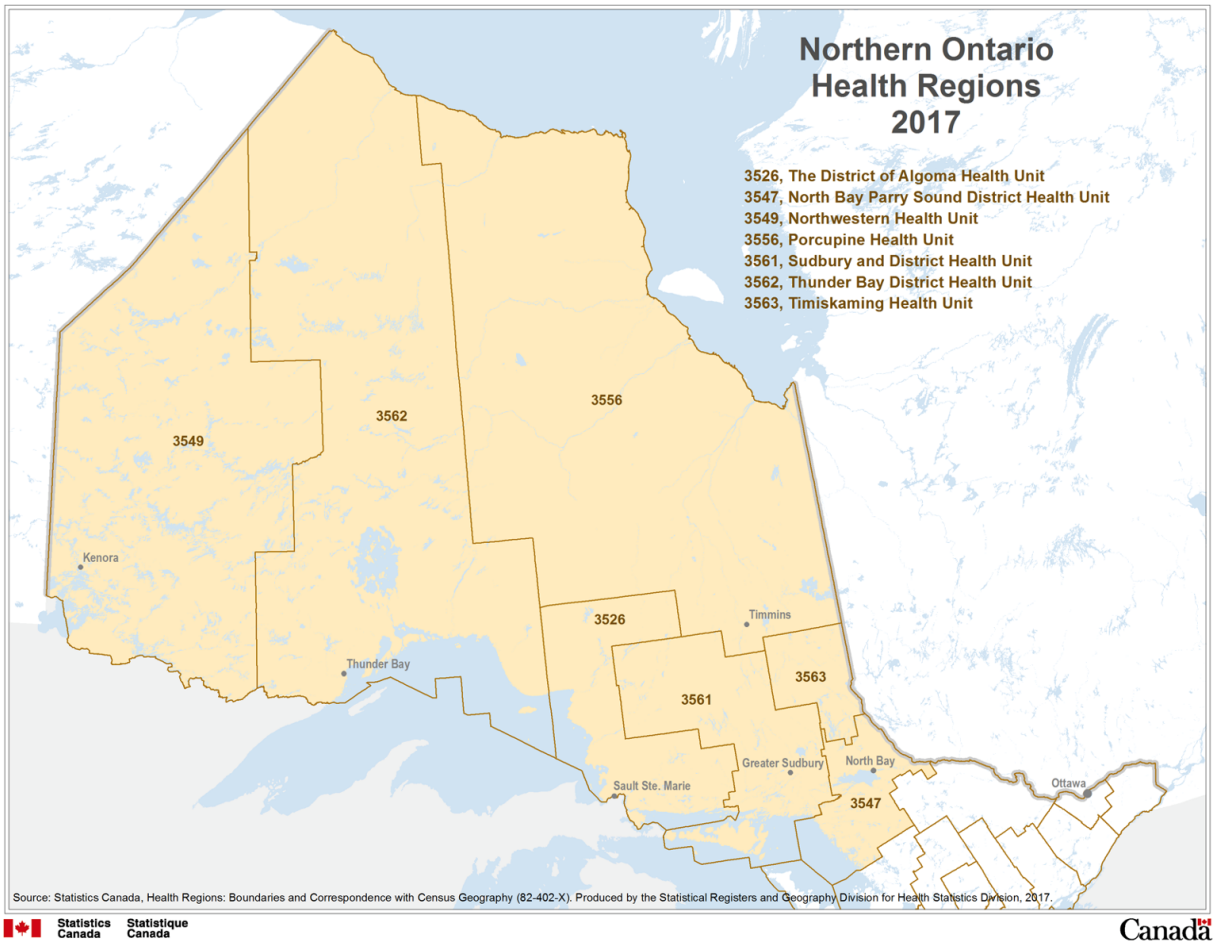

Figure 4.2: Northern Ontario Health Regions

Table 4.1 shows the number of healthcare workers by health region and the weekly demand for masks and gowns.

The total amount of supply available in the network was estimated to be almost double the total demand. We assume that supply is available from four health regions. The City of Ottawa Health Unit, Sudbury and District Health Unit, The City of Toronto Health Unit, and Windsor-Essex County Health Unit all produce their own supply of masks and gowns. We assume that Windsor also receives large shipments of masks from the United States and that Ottawa also receives large shipments of gowns each time period from Quebec. The supply available from each health region during each time period is shown in Table 4.2.

During the peak of the COVID-19 outbreak in New York City during the Spring of 2020, weekly PPE deliveries were being made to hospitals (Greater New York Hospital Association, 2020). Thus, we will consider the duration of a time period to be a week. In the numerical testing, we consider four total time periods or approximately one month.

According to Cerasis Inc. (2015), a standard freight trailer can hold 26 pallets, where a standard pallet is $48in$ by $40in$ (Freight Quote by C.H. Robinson, 2020). Since a box of surgical masks has dimensions $7.5in$ by $4.25in$ by $4in$ (North American Rescue, 2020), a pallet can hold approximately 972 product units and a transport truck can hold approximately $25,272$ product units.

According to Hooper and Murray (2018) the 2017 average truck transportation cost in the United States was \$1.691 USD/mile, which equates to approximately \$1.33 CAD/km. After adjusting for Canadian inflation (Statista, 2021), the average truck transportation cost would be \$1.42 CAD/km in 2021. For the test cases, two different carriers are used (Carrier A and Carrier B), however the cost per km for each carrier is considered to be the

Table 4.1: Weekly Demand per Health Region

Health Region	**Healthcare Workers**	**Mask Demand**	**Gown Demand**
The District of Algoma	4,475	1,790	4,475
Brant County	4,340	1,736	4,340
Chatham-Kent	3,580	1,432	3,580
Durham Regional	20,795	8,318	20,795
Eastern Ontario	6,760	2,704	6,760
Elgin-St. Thomas	3,150	1,260	3,150
Grey Bruce	5,915	2,366	5,915
Haldimand-Norfolk	3,765	1,506	3,765
Haliburton, Kawartha, Pine Ridge District	5,820	2,328	5,820
Halton Regional	16,530	6,612	16,530
City of Hamilton	21,745	8,698	21,745
Hastings and Prince Edward Counties	5,260	2,104	5,260
Huron County	1,775	710	1,775
Kingston, Frontenac and Lennox and Addington	9,350	3,740	9,350
Lambton	4,640	1,856	4,640
Leeds, Grenville and Lanark District	6,085	2,434	6,085
Middlesex-London	20,040	8,016	20,040
Niagara Regional Area	15,885	6,354	15,885
North Bay Parry Sound District	4,880	1,952	4,880
Northwestern	2,595	1,038	2,595
City of Ottawa	32,880	13,152	32,880
Oxford County	3,465	1,386	3,465
Peel Regional	37,400	14,960	37,400
Perth District	2,535	1,014	2,535
Peterborough County-City	5,375	2,150	5,375
Porcupine	3,055	1,222	3,055
Renfrew County and District	4,005	1,602	4,005
Simcoe Muskoka District	18,780	7,512	18,780
Sudbury and District	8,400	3,360	8,400
Thunder Bay District	6,795	2,718	6,795
Timiskaming	1,170	468	1,170
City of Toronto	84,365	33,746	84,365
Waterloo	16,020	6,408	16,020
Wellington-Dufferin-Guelph	8,970	3,588	8,970
Windsor-Essex County	15,260	6,104	15,260
York Regional	31,190	12,476	31,190
Total	**447,050**	**178,820**	**447,050**

Table 4.2: PPE Supply per Time Period

Health Region	**Mask Supply per Time Period**	**Gown Supply per Time Period**
City of Ottawa	12,400	662,300
Sudbury and District	10,400	22,600
City of Toronto	37,400	115,900
Windsor-Essex County	247,500	26,600
Total	**307,700**	**827,400**

same. The test cases also assume that there is route capacity available from each carrier on each route (i.e. $u_{ij}^r = 1 \ \forall i, j, r$). The cost to acquire one PPE unit of capacity on route $i - j$ (w_{ij}) is calculated by

$$\frac{(\textit{truckload cost/km})\,(\textit{road distance between } i \textit{ and } j)}{25,272 \textit{ product units per truck}}.$$

Road distances are calculated using Google Maps (2021) and are provided in Tables A.1, A.2, A.3, A.4, A.5, and A.6. The w_{ij} values are provided in Tables A.7, A.8, A.9, A.10, A.11, and A.12. The capacity for route $i - j$ per time period from carrier r (h_{ij}^r) is considered to be the demand per time period for health region j. For example, the District of Algoma Health Region requires a total of $6,265$ units of demand per time period. Thus, $h_{i,j}^r = 6,265 \ \forall i, r$, where $j = \textit{Algoma}$.

For the test cases, it is assumed that there is storage capacity available to be acquired from each carrier at each health region (i.e. $v_j^r = 1 \ \forall j, r$). At each health region, we estimate that Carrier A has storage capacity of $1,550$ cubic feet available from its existing network for $\$43,000$ per month. We estimate that Carrier B has $3,250$ cubic feet of storage capacity available from its existing network for $\$88,000$ per month at each health region. Since a box of masks measures $7.5in$ by $4.25in$ by $4in$ and a box of surgical masks and a box of medical gowns are considered to have the same dimensions, Carrier A has storage capacity for $21,000$ PPE units at each health region and Carrier B has $44,000$ units of

storage capacity available at each health region.

The cost required to distribute an additional unit of PPE during the second stage of the stochastic model is set to \$0.25 for all routes (i.e. $\gamma_{ij} = 0.25 \ \forall i, j$). This is approximately double the maximum unit distribution cost between health regions. Thus, it is more expensive to distribute a unit of PPE along a route during the second stage compared to the first stage. The cost recovered from removing a unit of PPE from a route during the second stage is assumed to be negligible and is set to \$0 for all routes (i.e. $\varphi_{ij} = 0 \ \forall i, j$).

4.1 Priority Values

A health region's priority corresponds to its need for PPE, which we will attempt to evaluate based on the total number of COVID cases, the number of COVID-related deaths, and the population density. Population density was included as places with high population density tend to have a higher rate of COVID-19 transmission (Rocklöv and Sjödin, 2020). The COVID-19 case and death counts used in the priority model are accurate as of June 22, 2020. Population density data is taken from the 2016 Census (Statistics Canada, 2020).

Some health units contain a large area of land with only one major city. As a result, population density can become skewed. For example, Sault Ste. Marie is part of The District of Algoma Health Unit, which covers a large area of $41,267 km^2$ and has a much lower population density ($2.7 people/km^2$) than the city of Sault Ste. Marie ($97 people/km^2$). Because of the large difference in population density, Sault Ste. Marie was considered to be its own destination city and the remaining area of The District of Algoma Health Unit as well as all COVID cases in the area were disregarded. This approach was also applied to the cities of Barrie, Greater Sudbury, Guelph, London, Mississauga, Ottawa, and Thunder Bay.

The set of Quebec Health Regions was used as a training data set with Quebec COVID-19 data taken from Quebec.ca (2021). For each predictor (total COVID-19 cases, total COVID-19-related deaths, and population density), the Quebec health regions were ranked in ascending order. The set of average rankings was then scaled so that the largest value in the set was 20. The scaled averages were considered to be the priority values for the training set and they were used as the dependent variable when determining the regression formulas. The Quebec regions and the scaled priority values are shown in Table 4.3.

Using the statistical computing software, R, seven linear regression models are obtained using different combinations of the predictors. The coefficient of determination, R^2, can be used to determine the quality of the model. However, as more parameters are added to the model, R^2 can never decrease. As Kutner et al. (2005) suggest, the adjusted coefficient of multiple determination, $R^2_{a,\mathcal{P}}$ is an alternative used for model selection which takes the number of parameters into account.

The parameters used for the seven different linear regression models and the corresponding $R^2_{a,\mathcal{P}}$ values are shown in Table 4.4. For each regression model, only the included parameters are used to calculate the average ranks. For example, for the model that considers only COVID-19 cases and COVID-19-related deaths as predictors, only the number of cases and the number of deaths are considered for the average rank.

Table 4.4: Parameters Used for Regression Models

COVID-19 Cases	**COVID-19 Deaths**	**Population Density**	$R^2_{a,\mathcal{P}}$
✓			0.41
	✓		0.30
		✓	0.29
✓	✓		0.59
✓		✓	0.42
	✓	✓	0.28
✓	✓	✓	0.66

Table 4.3: Quebec COVID-19 Data (accurate as of June 22, 2020)

Health Regions	**COVID-19 Cases (rank)**	**COVID-19 Deaths (rank)**	**Population Density (rank)**	**Average Rank**	**Scaled Average**
Region de l'Abitibi-Temiscamingue	172 (6)	4 (6)	2.5 (4)	$5.3\bar{3}$	5.93
Region de l'Estrie	959 (11)	25 (9)	37.1 (13)	11	$12.2\bar{2}$
Region de l'Outaouais	576 (10)	33 (11)	12.4 (10)	$10.2\bar{2}$	11.48
Region de la Capitale-Nationale	1806 (12)	171 (12)	38.8 (14)	$12.6\bar{6}$	14.07
Region de la Chaudiere-Appalaches	514 (9)	8 (7)	27.9 (11)	9	10
Region de la Cote-Nord	119 (5)	0 (1)	0.4 (3)	3	$3.3\bar{3}$
Region de la Gaspesie - Iles-de-la-Madeline	187 (7)	9 (7)	4.4 (7)	$7.3\bar{3}$	18.15
Region de la Mauricie et du Centre-du-Quebec	2041 (13)	210 (15)	11.9 (9)	$12.3\bar{3}$	13.70
Region de la Monteregie	7750 (17)	557 (16)	157.3 (16)	$16.3\bar{3}$	18.15
Region de la Lanaudiere	4150 (15)	206 (14)	39.8 (15)	$14.6\bar{6}$	16.30
Region de Laval	5750 (16)	659 (17)	1710.9 (17)	$16.6\bar{6}$	18.52
Region de Montreal	27, 057 (18)	3329 (18)	3889.8 (18)	18	20
Region des Laurentides	3312 (14)	178 (13)	28.4 (12)	13	$14.4\bar{4}$
Region du Bas-Saint-Laurent	56 (4)	2 (5)	8.9 (8)	$5.6\bar{6}$	6.30
Region du Nord-du-Quebec	8 (1)	0 (1)	0.05 (2)	$1.3\bar{3}$	1.48
Region du Nunavik	17 (3)	0 (1)	0.03 (1)	$1.6\bar{6}$	1.85
Region du Saguenay - Lac-Saint-Jean	330 (8)	26 (10)	2.8 (5)	$7.6\bar{6}$	8.52
Region des Terres-Cries-de-la-Baie-James	10 (2)	0 (1)	3.1 (6)	3	$3.3\bar{3}$

The model with all three parameters has the highest adjusted coefficient value. The summary table for this regression model is shown in Table 4.5.

Table 4.5: Priority Regression Summary

Coefficients	Estimate	p-value
(Intercept)	6.68312	2.46e−05
Case Count	0.004344	0.000953
Death Count	-0.038329	0.003977
Population Density	0.006191	0.105239

Since the population density parameter is not significant, it is removed in Table 4.6.

Table 4.6: Priority Regression Summary Without Population Density

Coefficient	Estimate	p-value
(Intercept)	7.0043989	1.83e−05
Case Count	0.0035217	0.00284
Death Count	-0.0242457	0.00914

We find that both remaining predictors are significant. However, Table 4.7 shows the correlation between all three original predictors and we see that the three predictors are highly correlated.

Table 4.7: Correlation Between Priority Predictors

	Case Count	Death Count	Population Density
Case Count	1.00	0.99	0.93
Death Count	0.99	1.00	0.96
Population Density	0.93	0.96	1.00

Thus, there is multicollinearity in both regression models and we will use the COVID-19 case counts as the only predictor. The resulting linear regression formula is

$$priority = 8.7379083 + (0.0005969 * cases). \tag{4.1}$$

The regression table from R is shown in Table 4.8.

Table 4.8: Priority Regression Summary Without Population Density and Death Count

Coefficients	Estimate	p-value
(Intercept)	8.7379083	2.45e−06
Case Count	0.004344	0.00395

The Ontario Health Region priorities as calculated by the regression formula are shown in Tables 4.9 and 4.10. The τ parameter was set to $\max_{ij} \{ w_{ij} \}$ (i.e. $\tau = 0.13$).

4.2 Pandemic Uncertainty

The two-stage stochastic model with recourse considers the possibility of increased pandemic severity happening in some regions. The Government of Ontario has five risk categories for COVID-19 public health measures: Prevent, Protect, Restrict, Control, and Lockdown (Ontario.ca, 2020a). Ontario health regions are assigned categories based on the number of COVID-19 cases. People in Lockdown regions are most at-risk of infection and people in Prevent regions are at the lowest risk of infection. The higher-risk categories also have more business restrictions and require more PPE.

According to Public Health Ontario (2020), two weeks of decreasing COVID-19 cases in a region are required for the region to improve to the next category. Public Health Ontario (2020) also describes the United States Center for Disease Control (CDC) conditions for being classified as a high-risk country. A high-risk country is defined as one which has more than 500 new daily cases and a daily incidence rate of more than three new cases per $100,000$ people.

The test cases combine and modify Public Health Ontario's and the CDC's conditions

Table 4.9: Ontario Health Region Priorities, Part 1*

Health Regions	COVID-19 Cases	COVID-19 Deaths	Population Density	Priority	COVID-19 Data Source
Barrie	174	14	219.4	8.72	simcoemuskokahealth.org
Brant County Health Unit	121	4	119.5	8.69	bchu.org
Chatham-Kent Health Unit	157	1	14.3	8.71	ckphu.com
City of Hamilton Health Unit	802	43	544.9	9.09	hamilton.ca
City of Toronto Health Unit	13856	1039	4334.4	16.88	toronto.ca
Durham Regional Health Unit	1671	180	255.9	9.61	app.powerbi.com
Elgin-St.Thomas Health Unit	39	1.90	47.3	8.64	swpublichealth.ca
Greater Sudbury	61	1.82	42	8.65	phsd.ca
Grey Bruce Health Unit	106	0	18.8	8.69	publichealthgreybruce.on.ca
Guelph	198	11	256.1	8.73	wdgpublichealth.ca
Haldimand-Norfolk Health Unit	445	32	38.4	8.88	hnhu.org
Haliburton et al. Health Unit	189	32	19.8	8.73	hkpr.on.ca
Halton Regional Health Unit	798	25	568.9	9.09	halton.ca
Hastings and Prince Edward Counties Health Unit	43	5	22.5	8.64	hpepublichealth.ca
Huron County Health Unit	13	0	17.4	8.62	hpph.ca
Kingston et al. Health Unit	64	0	29.2	8.65	kflaph.ca
Lambton Health Unit	285	25	42.2	8.79	lambtonpublichealth.ca
Leeds et al. Health Unit	352	52	26.4	8.83	healthunit.org
London	566	53.15	185.6	8.95	healthunit.com

*COVID-19 Data Accurate as of June 22, 2020.

Table 4.10: Ontario Health Region Priorities, Part 2*

Health Regions	COVID-19 Cases	COVID-19 Deaths	Population Density	Priority	COVID-19 Data Source
Mississauga	2564	216	2467.6	10.14	peelregion.ca
Niagara Regional Area Health Unit	741	61	241.5	9.06	stcatharinesstandard.ca
North Bay Parry Sound District Health Unit	30	1	7.3	8.63	myhealthunit.ca
Northwestern Health Unit	30	0	0.4	8.63	nwhu.on.ca
Ottawa	2056	260	272.5	9.84	ottawapublichealth.ca
Oxford County Health Unit	43	2.10	54.4	8.64	swpublichealth.ca
Perth District Health Unit	41	5	34.6	8.64	hpph.ca
Peterborough County-City Health Unit	95	2	35.9	8.67	peterboroughpublichealth.ca
Porcupine Health Unit	67	8	0.3	8.66	porcupinehu.on.ca
Renfrew County and District Health Unit	25	1	6.9	8.63	rcdhu.com
Sault Ste. Marie	19	0	97	8.63	algomapublichealth.com
The Eastern Ontario Health Unit	163	11	38.2	8.71	eohu.ca
Thunder Bay Region	66	0.73	47.6	8.65	tbdhu.com
Timiskaming Health Unit	18	0	2.3	8.63	timiskaminghu.com
Waterloo Health Unit	1258	115	390.9	9.37	regionofwaterloo.ca
Windsor-Essex County Health Unit	1329	68	215.5	9.41	wechu.org
York Regional Health Unit	2857	236	629.9	10.32	york.ca

*COVID-19 Data Accurate as of June 22, 2020.

for COVID-19 risk. We consider a region to be at high-risk for transmissibility if it has an average incidence rate of greater than three over the past week and if the number of new COVID-19 cases has increased in the past week. The condition of having more than 500 new cases, as recommended by the CDC, was not used because we are dealing with individual Ontario health regions and that recommendation was made for entire countries. For example, a health region is said to be at high-risk at time t for our model if the incidence at time $t-1$ is greater than three and if the number of cases in the region has increased from time periods $t-2$ to $t-1$. If the high-risk conditions are not met, the region is considered to be at low-risk for transmissibility. A region's risk level remains constant for all time periods. Thus, a region in high-risk during the first time period will be at high-risk for all time periods in the model.

To determine the probability that a region would be at high-risk for the next time period, logistic regression was used to predict high-risk occurrence in the next time period from the region's incidence rate during the current time period. For each week between October 15, 2020 and November 11, 2020, the week's high-risk outcome and the previous week's average incidence rates were used in the regression calculations. Daily COVID-19 case count data for Huron County Health Unit and Perth District Health Unit was presented together, thus the two health regions were combined into one health region for the logistic regression calculations. The same applies for the Oxford County and the Elgin-St. Thomas health units. Daily COVID-19 case counts used in the stochastic model were obtained from Ontario.ca (2020b) and were taken on November 11, 2020. The daily numbers of new COVID-19 cases by health region are provided in Tables A.13, A.14, A.15, A.16, A.17, A.18, A.19, A.20, A.21, A.22, A.23, and A.24. Population data used to calculate incidence rates was obtained from the 2016 Census (Statistics Canada, 2020) on November 15, 2020. The health region populations are given in Table A.25.

The logistic regression formula obtained from R is:

$$\hat{p} = \frac{exp(-3.6164 + 0.6752X)}{1 + exp(-3.6164 + 0.6752X)} \tag{4.2}$$

where $\hat{p}$ is the probability that a region will be in high-risk during the next time period, and X is the region's average daily incidence rate during the current time period. The regression table from R is shown in Table 4.11. From the p-values, we can see that the predictor is significant. The high-risk probabilities for each health region are shown in Table 4.12.

Table 4.11: Pandemic Progression Regression Table

	Estimate	p-value
(Intercept)	-3.6164	1.58e−11
Previous Week's Incidence Rate	0.6752	1.99e−08

There are 36 health regions in Ontario, as shown in Figures 4.1 and 4.2. To simplify the model, health regions were grouped together based on geographic location and high-risk probability to form clusters. All health regions within a cluster are considered to have the same COVID-19 risk level. For example, if a cluster is at high-risk of COVID-19 transmission, all health regions within the cluster are at high-risk of COVID-19 transmission. Durham Regional Health Unit and Windsor-Essex County Health Unit and District Health Unit do not have similar high-risk probabilities as other health units which are geographically near them. As such, Durham and Windsor-Essex each formed its own cluster. To calculate the high-risk probabilities for each cluster, aggregate COVID-19 incidence rates were used with logistic regression. The logistic regression formula for the health region clusters is:

$$\hat{p} = \frac{exp(-3.7778 + 0.6561X)}{1 + exp(-3.7778 + 0.6561X)} \tag{4.3}$$

Table 4.12: Health Region High-Risk Probabilities

Health Unit	**High-Risk Probability for November 12-18**
Peel Regional Health Unit	$> 99\%$
City of Toronto Health Unit	$> 99\%$
York Regional Health Unit	96%
City of Hamilton Health Unit	83%
Halton Region Health Department	81%
Niagara Regional Area Health Unit	70%
Waterloo Health Unit	67%
Durham Regional Health Unit	54%
Huron County-Perth District Health Unit	53%
City of Ottawa Health Unit	51%
Windsor-Essex County Health Unit	44%
Wellington-Dufferin-Guelph Health Unit	35%
Brant County Health Unit	33%
Eastern Ontario Health Unit	29%
Middlesex-London Health Unit	29%
Sudbury & District Health Unit	28%
Simcoe Muskoka District Health Unit	18%
Oxford County - Elgin-St. Thomas Health Unit	17%
Chatham-Kent Health Unit	16%
Haldimand-Norfolk Health Unit	13%
Thunder Bay District Health Unit	11%
Grey Bruce Health Unit	8%
The District of Algoma Public Health Unit	7%
Northwestern Health Unit	6%
Leeds et al. District Health Unit	5%
Peterborough County-City Health Unit	5%
Kingston et al. Health Unit	5%
Renfrew County and District Health Unit	5%
Lambton Health Unit	4%
North Bay Parry Sound District Health Unit	4%
Porcupine Health Unit	4%
Haliburton et al. Health Unit	3%
Hastings and Prince Edward Counties Health Unit	3%
Timiskaming Health Unit	3%

where $\hat{p}$ is the expected probability that a cluster will be in high-risk during the next time period, and X is the cluster's incidence rate from the current time period. The regression table from R is shown in Table 4.13. From the p-values, we can see that the predictor is significant. We note that the pandemic progression predictions could also be done using a Susceptible-Infected-Removed (SIR) model. We will use this regression model to predict the high-risk probabilities for the time period of November 12-18, 2020. A region's risk level for November 12-18 remains the same for all time periods in the stochastic program. The resulting eleven clusters, their high-risk probabilities for November 12-18 and the health regions they comprise are shown in Table 4.14. A map of the health region clusters is given in Figure 4.3.

Table 4.13: Pandemic Progression by Cluster Regression Table

	Estimate	p-value
(Intercept)	-3.7778	0.000126
Previous Week's Incidence Rate	0.6561	0.000908

As Martin-Olalla (2020) notes, large COVID-19 outbreaks occurring in neighbouring regions are independent events. Thus, we will consider the risk levels at each cluster to be independent of one another. We will model high-risk uncertainty with a two-stage scenario tree as shown in Figure 4.4. Each leaf node in the tree represents a scenario in which a different combination of clusters are at high-risk of COVID-19 transmission. Since the eleven Ontario health region clusters can be classified as either in high-risk or in low-risk, we would have $2^{11} = 2048$ scenarios. To reduce the number of scenarios, the demand for all clusters with high-risk probabilities of greater than 99% or less than 1% are considered to be deterministic. Clusters with high-risk probabilities greater than 99% are considered certain to be at high-risk. Clusters with high-risk probabilities less than 1% are considered certain to be at low-risk. Only the GTA fits this criteria. Thus, the GTA is considered to have a high-risk probability of 100% for the

Table 4.14: Health Region Clusters

Cluster	**High-Risk Probability for Nov 12-18**	**Health Region 1**	**Health Region 2**	**Health Region 3**	**Health Region 4**	**Health Region 5**
Greater Toronto Area (GTA)	$> 99\%$	City of Toronto	York Regional	Peel Regional		
GTA Suburbs	74%	City of Hamilton	Halton Regional	Niagara Regional Area		
Durham	48%	Durham Regional				
Central Ontario	46%	Waterloo	Huron County	Perth District	Wellington-Dufferin-Guelph	Brant County
Eastern Ontario	41%	City of Ottawa	Eastern Ontario			
Windsor-Essex	38%	Windsor-Essex County				
Southern Ontario	16%	Middlesex-London	Oxford County	Elgin - St. Thomas	Chatham-Kent	Lambton
Georgian Bay	12%	Simcoe-Muskoka District	Grey Bruce			
North Shore	8%	Sudbury and District	District of Algoma	Renfrew County and District	North Bay Parry Sound District	Timiskaming
Northern Ontario	6%	Thunder Bay District	Northwestern	Porcupine		
Peterborough	4%	Leeds et al.	Peterborough County-City	Kingston et al.	Haliburton et al.	Hastings and Prince Edward Counties

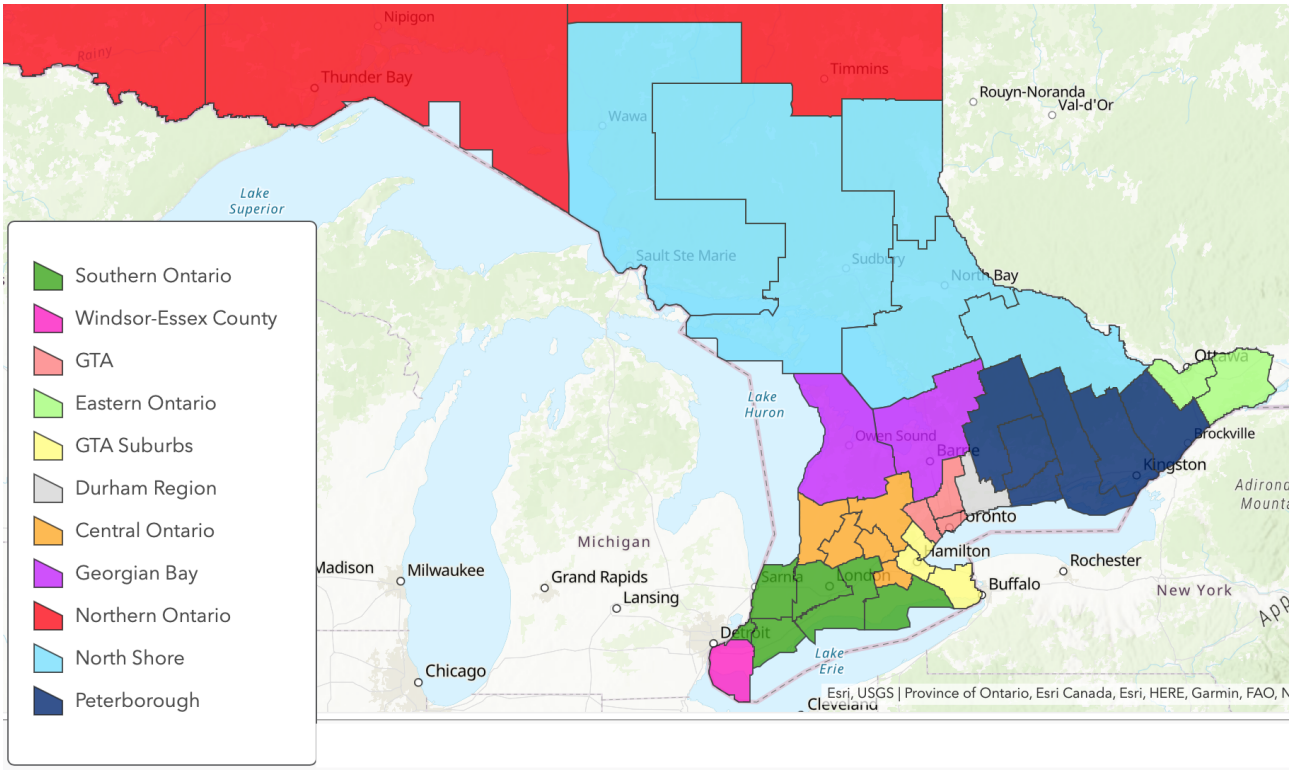

Figure 4.3: Health Region Clusters Map

next time period. This leaves $2^{10} = 1024$ scenarios remaining. To find the probability of each scenario, the probabilities of each cluster being in the desired risk-level are multiplied together. For example, the probability of the scenario where the GTA Suburbs cluster is at high risk and all other groups (other than the GTA) are at low-risk is $(0.74)\,(1-0.48)\,(0.46)\,(1-0.41)\,(1-0.38)\,(1-0.16)\,(1-0.12)\,(1-0.8)\,(1-0.6)\,(1-0.4) = 0.048$.

According to an international study conducted by Tabah et al. (2020), 4% of surgical masks are being washed or reused in healthcare settings. Similarly, 11% of full sleeve waterproof gowns are being washed or reused. When a region is in high-risk, mask demand will be increased by 4% and gown demand will be increased by 11%. The weekly PPE

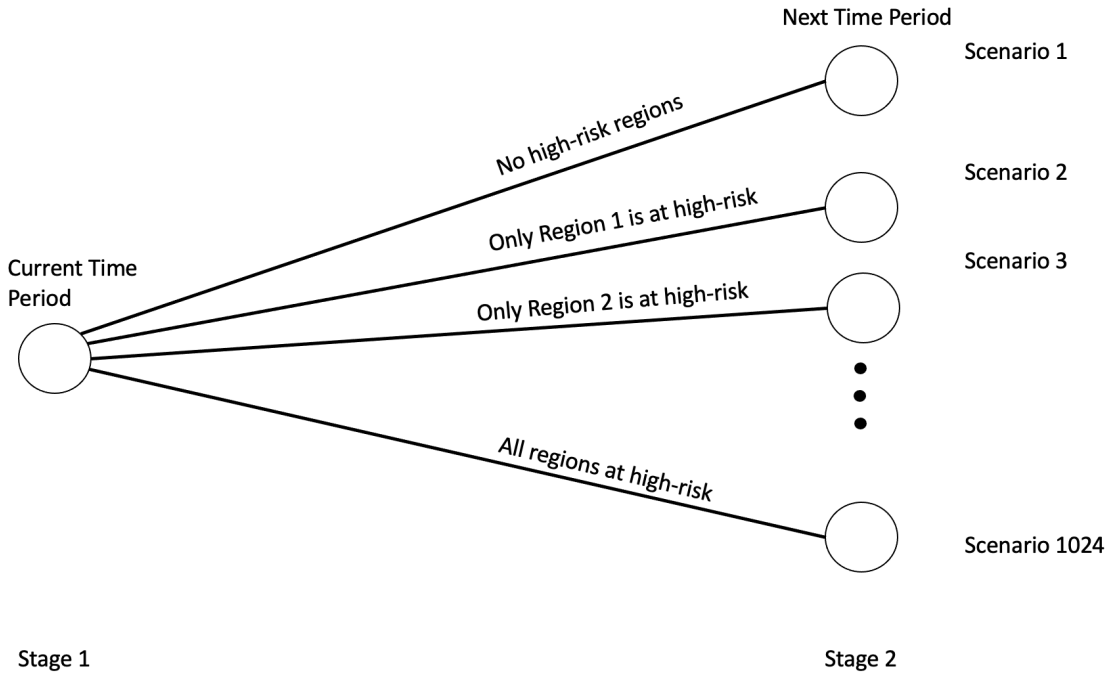

Figure 4.4: COVID-19 High-Risk Scenario Tree. There are 1024 different combinations of scenarios that can occur.

demand for each health region during high-risk time periods is shown in Table 4.15.

Table 4.15: Weekly Demand for Health Regions During High-Risk Time Periods

Health Region	**High-Risk Mask Demand**	**High-Risk Gown Demand**
The District of Algoma	1,862	4,967
Brant County	1,805	4,817
Chatham-Kent	1,489	3,974
Durham Regional	8,651	23,082
Eastern Ontario	2,812	7,504
Elgin-St. Thomas	1,310	3,497
Grey Bruce	2,461	6,566
Haldimand-Norfolk	1,566	4,179
Haliburton, Kawartha, Pine Ridge District	2,421	6,460
Halton Regional	6,876	18,348
City of Hamilton	9,046	24,137
Hastings and Prince Edward Counties	2,188	5,839
Huron County	738	1,970
Kingston, Frontenac and Lennox and Addington	3,890	10,379
Lambton	1,930	5,150
Leeds, Grenville and Lanark District	2,531	6,754
Middlesex-London	8,337	22,244
Niagara Regional Area	6,608	17,632
North Bay Parry Sound District	2,030	5,417
Northwestern	1,080	2,880
City of Ottawa	13,678	36,497
Oxford County	1,441	3,846
Peel Regional	15,558	41,514
Perth District	1,055	2,814
Peterborough County-City	2,236	5,966
Porcupine	1,271	3,391
Renfrew County and District	1,666	4,446
Simcoe Muskoka District	7,812	20,846
Sudbury and District	3,494	9,324
Thunder Bay District	2,827	7,542
Timiskaming	487	1,299
City of Toronto	35,096	93,645
Waterloo	6,664	17,782
Wellington-Dufferin-Guelph	3,732	9,957
Windsor-Essex County	6,348	16,939
York Regional	12,975	34,621
Total	**185,973**	**496,226**

Chapter 5

Numerical Testing

The proposed models were compared using the data described in the previous chapter. All tests were conducted using Python 3.8 with Gurobi 9 and were executed on MacOS i7 with 16GB RAM. The two-stage stochastic model with recourse is approximated with sample average approximation and solved with the same parameters using Benders decomposition. The Benders decomposition algorithm was allowed to run until the optimality gap was within 1% for a maximum run time of one hour. For the sample average approximation algorithm, we used $M = 10$ samples each of size $N = 10$. Each SAA problem within the sample average approximation algorithm, was solved using Benders decomposition and was allowed to solve for a maximum of five minutes. When solving the second stage in the final sample average approximation step (2.4), a sample size of $N' = 20$ was used. For comparison, the priority model was also solved using the same parameters and was allowed to solve for one hour. Table 5.1 compares the solutions of the three models.

All three models solved to within 0.31% of optimality. The solutions obtained from Benders decomposition and sample average approximation are very similar and the first-stage

Table 5.1: Method Comparison

	Benders	**SAA**	**Priority**
Solution Time (min)	23	56	60
Gap	0.31%	0.06%	0.25%
Objective Value	4,141,708	4,146,894	4,127,139

solutions are identical. All stochastic model results presented are the Benders decomposition solutions. Figures 5.1 and 5.2 show the first-stage distribution of mask supply, where thicker lines indicate more units of PPE being distributed than thinner lines. Since, the majority of mask supply originates from Windsor, large quantities of masks are transported from Windsor to other Southern Ontario locations (such as Hamilton, London, and Waterloo) before being distributed to the rest of the province. For example, masks arrive in Timiskaming using the following path: *Windsor* $\rightarrow$ *Hamilton* $\rightarrow$ *Peel* $\rightarrow$ *Simcoe* $\rightarrow$ *Timiskaming*. Figures 5.3 and 5.4 show the gown distribution from the sample average approximation solution. Similarly to most of the mask supply coming from Windsor, the majority of gown supply originates in Ottawa. From Ottawa, the large quantities of gown supply are distributed to the rest of the province.

Warehouse capacity is acquired at every location and often from both carriers. Acquiring capacity at such a large number of warehouses is due to the excess supply available and the relatively small capacity available at each warehouse compared with the total demand.

We will denote the scenario that is most likely to occur as Scenario A. This scenario occurs with probability 4.8% and considers the GTA and the GTA Suburbs as high-risk COVID-19 clusters. All remaining health region clusters are at low-risk. Table 5.2 shows the change in demand and in PPE received for high-risk health regions between the first stage of the stochastic program and Scenario A. The values in Table 5.2 represent the combined PPE units between all products and time periods, however the change in PPE

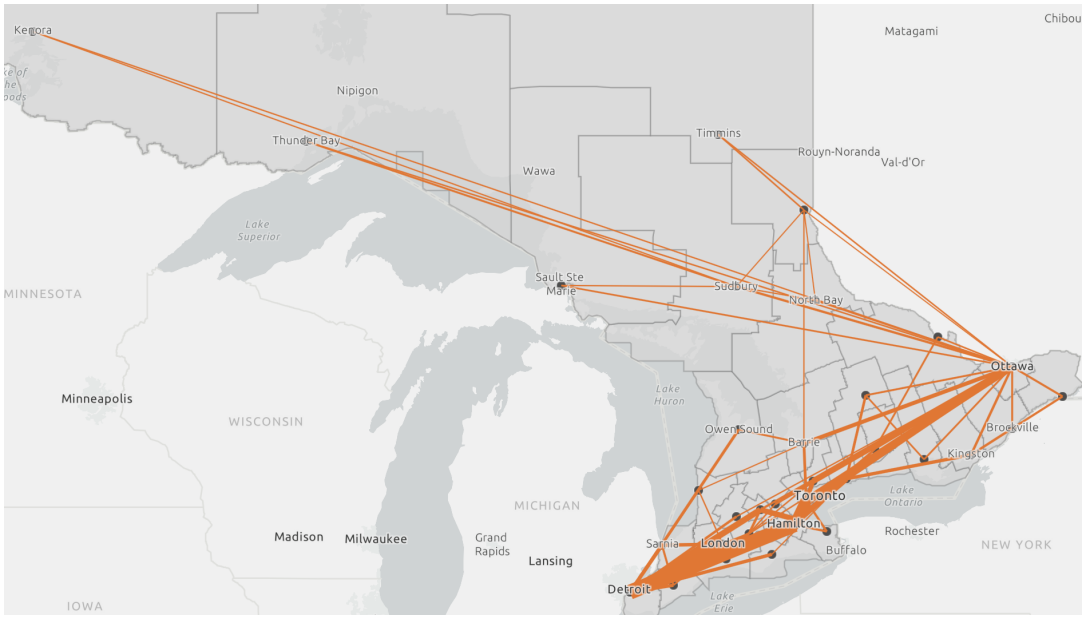

Figure 5.1: Mask Distribution during the First Stage

Figure 5.2: Southern Ontario Mask Distribution during the First Stage

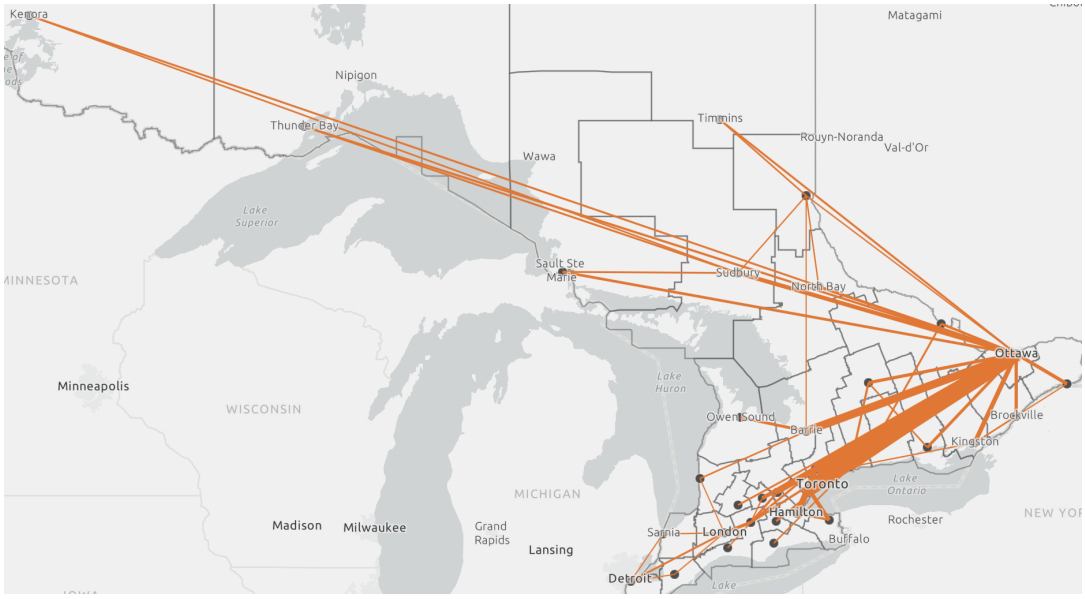

Figure 5.3: Gown Distribution during the First Stage

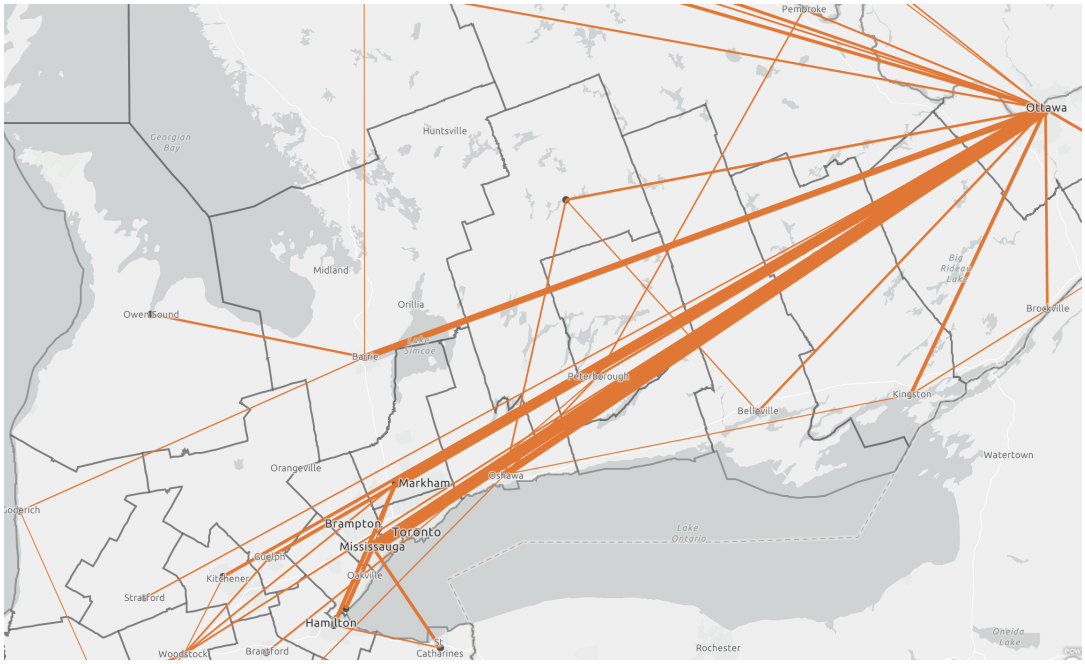

Figure 5.4: Southern Ontario Gown Distribution during the First Stage

received does not include inventory amounts. Even though six health regions have increased demand during this scenario, only three regions (Peel, York, and Hamilton) receive all or more than the extra demand from distribution. And only York receives slightly more PPE than demand, thus close to the minimum amount of demand necessary is rerouted during the second stage. Regions whose increased distribution from rerouting is less than the increase in demand satisfy this extra demand using existing inventory.

Table 5.2: PPE Changes Under Scenario A

Health Region Cluster	**Health Regions**	**Demand Increase Between First Stage and Second Stage Scenario A**	**Total Change in PPE Received Between First Stage and Scenario A**
GTA	**Peel**	18,852	18,852
	Toronto	42,524	21,506
	York	15,724	16,536
GTA Suburbs	**Halton**	8,336	-555
	Hamilton	10,960	10,960
	Niagara	8,012	-10,695

The two-stage stochastic model with recourse was solved directly to verify the results obtained from Benders decomposition and sample average approximation. For small test cases, the solutions matched. For the test cases shown in this chapter, the stochastic program could not be solved directly due to a lack of memory.

The priority model generated similar results to the first stage of the stochastic program. Since there is excess supply, all demand at each region is fulfilled (i.e. $\rho_i^{pt} = 1 \ \forall i, p, t$).

5.1 Pandemic Severity Becomes Known

The two-stage stochastic model with recourse considers 1024 potential scenarios to handle the pandemic uncertainty. We make predictions regarding which regions are at high-risk

for COVID-19 infection and which regions are at low-risk for the week of November 12 - November 18, 2020. Looking back, we now know the actual severity of the pandemic for this time period. Using our high-risk definition of: an incidence rate greater than three over the past week and an increasing case count from the prior week, we calculate that five health region clusters would have been at high-risk during the week of November 12 - November 18, 2020 as shown in Table 5.3.

As shown in Table 5.4, the sum of net incoming PPE across all time periods at each health region matches or exceeds the required demand for the realized scenario. Net incoming PPE consists of the outgoing distributed PPE subtracted from the sum of the supply and incoming PPE distribution. For a scenario s, the formula to calculate net incoming PPE for each health region j and for each product p is as follows:

$$\sum_{t}\sum_{i}\left(\alpha_{ij}^{pt}+m_{ij}^{pts}-n_{ij}^{pts}\right)-\sum_{t}\sum_{k}\left(\alpha_{jk}^{pt}+m_{jk}^{pts}-n_{jk}^{pts}\right)+\sum_{t}g_{j}^{pt} \tag{5.1}$$

Excess PPE is stored as inventory using acquired warehouse capacity. Thus, our two-stage stochastic model with recourse is able to completely satisfy the demand given by the actual pandemic severity level.

Table 5.3: Actual Risk Levels of Health Region Groupings Risk Levels for Nov 12 - Nov 18, 2020

High-Risk Clusters during Nov 12 - Nov 18	**Low-Risk Clusters during Nov 12 - Nov 18**
GTA	GTA Suburbs
Durham	Southern Ontario
Windsor-Essex	Eastern Ontario
Central Ontario	North Shore
Georgian Bay	Peterborough
	Northern Ontario

Table 5.4: PPE Received for Second-Stage Realization

Health Region	Risk Level	Required Mask Demand	Net Incoming Masks	Excess Masks	Required Gown Demand	Net Incoming Gowns	Excess Gowns
Algoma	Low	7,160	7,160	0	17,900	82,900	65,000
Brant	High	7,224	42,252	35,028	19,272	27,700	8,428
Chatham	Low	5,728	70,728	65,000	14,320	14,320	0
Durham	High	34,604	34,604	0	92,332	157,332	65,000
Eastern	Low	10,816	10,816	0	27,040	90,223	63,183
Elgin	Low	5,040	68,870	63,830	12,600	12,600	0
GreyBruce	High	9,844	18,046	8,202	26,264	59,919	33,655
Haldimand	Low	6,024	45,968	39,944	15,060	19,116	4,056
Haliburton	Low	9,312	9,312	0	23,280	88,280	65,000
Halton	Low	26,448	26,448	0	66,120	118,860	52,740
Hamilton	Low	34,792	34,792	0	86,980	102,236	15,256
Hastings	Low	8,416	8,416	0	21,040	81,792	60,752
Huron	High	2,956	32,268	29,312	7,884	16,437	8,553
Kingston	Low	14,960	14,960	0	37,400	102,400	65,000
Lambton	Low	7,424	72,424	65,000	18,560	18,560	0
Leeds	Low	9,736	9,736	0	24,340	84,561	60,221
Middlesex	Low	32,064	97,064	65,000	80,160	80,160	0
Niagara	Low	25,416	25,416	0	63,540	127,460	63,920
NorthBay	Low	7,808	7,808	0	19,520	40,520	21,000
Northwestern	Low	4,152	4,152	0	10,380	54,380	44,000
Ottawa	Low	52,608	52,608	0	131,520	196,520	65,000
Oxford	Low	5,544	10,366	4,822	13,860	30,038	16,178
Peel	High	62,236	62,236	0	166,056	231,056	65,000
Perth	High	4,220	46,428	42,208	11,256	30,952	19,696
Peterborough	Low	8,600	8,600	0	21,500	86,500	65,000
Porcupine	Low	4,888	4,888	0	12,220	52,648	40,428
Renfrew	Low	6,408	6,408	0	16,020	64,771	48,751
Simcoe	High	31,252	31,252	0	83,384	148,384	65,000
Sudbury	Low	13,440	13,440	0	33,600	98,600	65,000
Thunderbay	Low	10,872	10,872	0	27,180	71,180	44,000
Timiskaming	Low	1,872	1,872	0	4,680	25,680	21,000
Toronto	High	140,384	140,384	0	374,584	435,557	60,973
Waterloo	High	26,660	42,978	16,318	71,132	99,670	28,538
Wellington	High	14,928	14,928	0	39,828	100,002	60,174
Windsor	High	25,396	90,396	65,000	67,756	67,756	0
York	High	51,904	51,904	0	138,484	190,530	52,046

5.2 Priority Value Sensitivity Analysis

In order to test how PPE is distributed given insufficient supply to satisfy all demand, test cases are performed with the priority model using reduced supply values, as provided in Table 5.5. With the reduced supply, no warehouse capacity is acquired as there is no excess PPE to be stored as inventory. Figure 5.5 shows the priority value for each health region and Figure 5.6 shows the total amount of PPE received and the total demand across all products and time periods for each health region. The amount of PPE received is calculated as the outgoing PPE distribution subtracted from the sum of the PPE supply and the incoming PPE distribution. Despite receiving significantly more PPE than any other region and having the largest priority value, Toronto does not necessarily receive a large proportion of its demand.

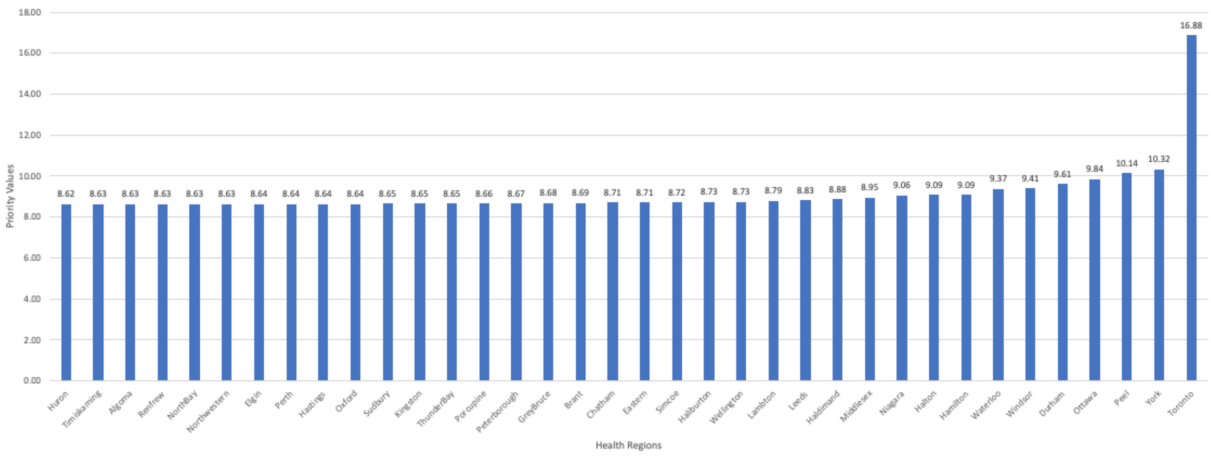

Figure 5.5: Health Region Priority Values

Figure 5.7 shows the average proportion of mask demand received for each health region across all time periods. The same proportions are mapped in Figures 5.8 and 5.9, where larger circles represent larger proportions of demand received. Many health regions receive all or a large proportion of their demand, however, Toronto has the largest priority value

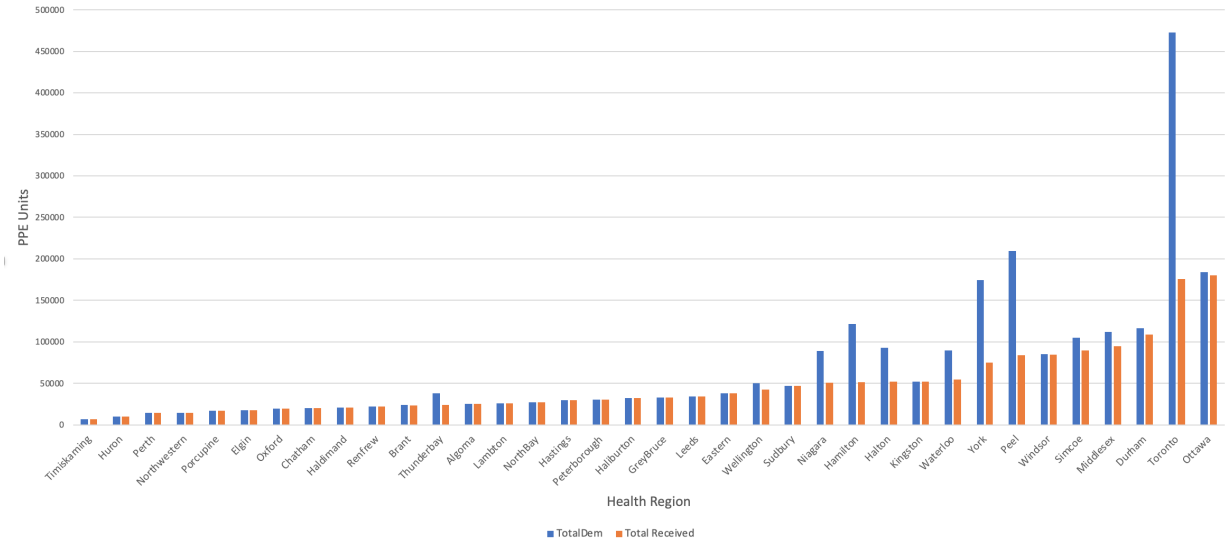

Figure 5.6: Total PPE Received by Health Region

and receives only 60% of its demand.

Figure 5.10 shows the average proportion of gown demand received for each health region across all time periods and Figures 5.11 and 5.12 show the maps of the same proportions. Many health regions with large priority values receive very small proportions of their gown demand. For example, York and Peel have the second and third largest priority values, respectively, however they each only receive 2% of their demand. Toronto, with by far the largest priority value, receives only 58% of its demand.

Table 5.5: Reduced PPE Supply

Health Region	**Mask Supply**	**Gown Supply**
Ottawa	42,400	96,200
Sudbury	9,300	21,600
Toronto	20,200	48,900
Windsor	86,200	76,500
Total	**158,160**	**190,218**

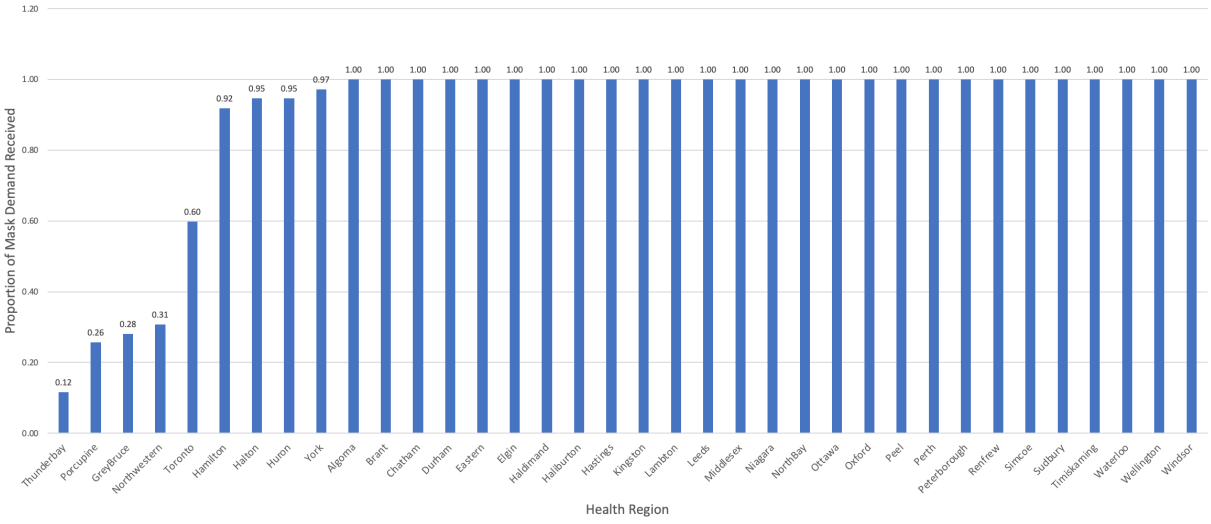

Figure 5.7: Average Proportion of Mask Demand Received Across all Time Periods

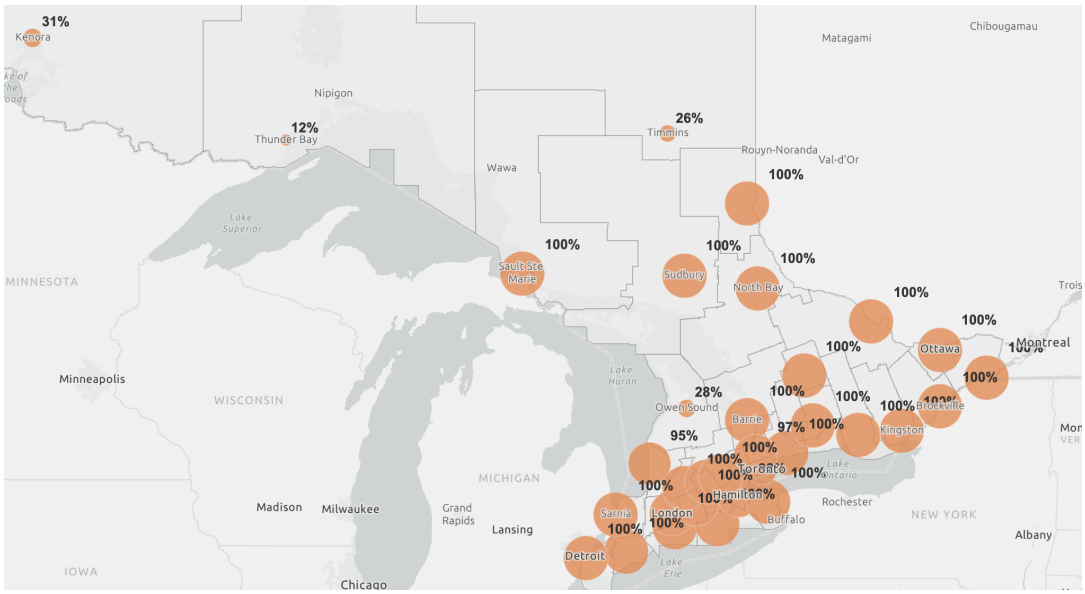

Figure 5.8: Map of Average Proportion of Mask Demand Received Across all Time Periods

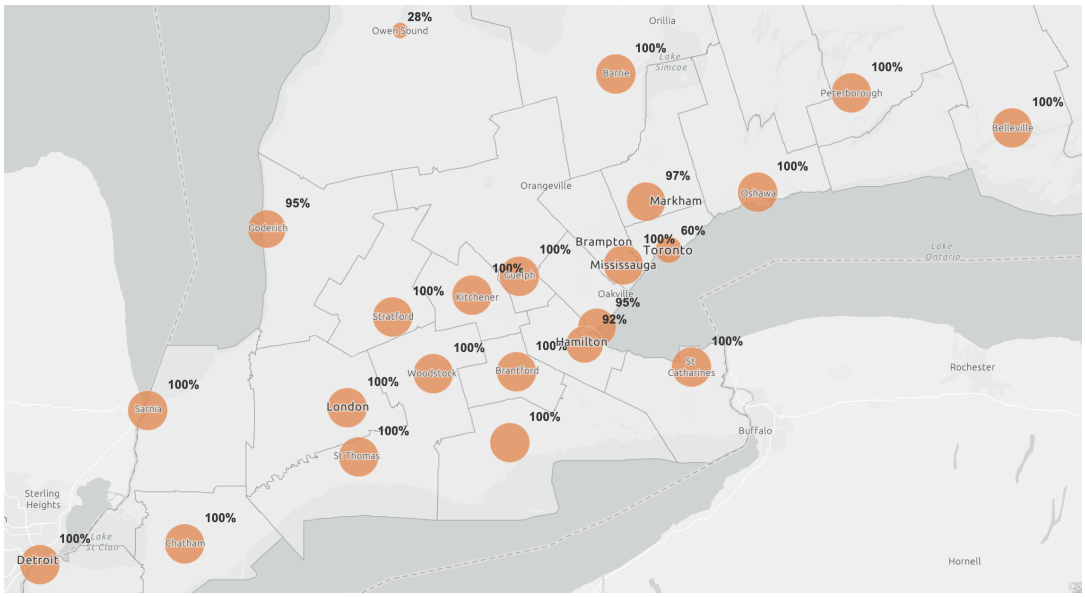

Figure 5.9: Map of Average Proportion of Mask Demand Received Across all Time Periods in Southern Ontario

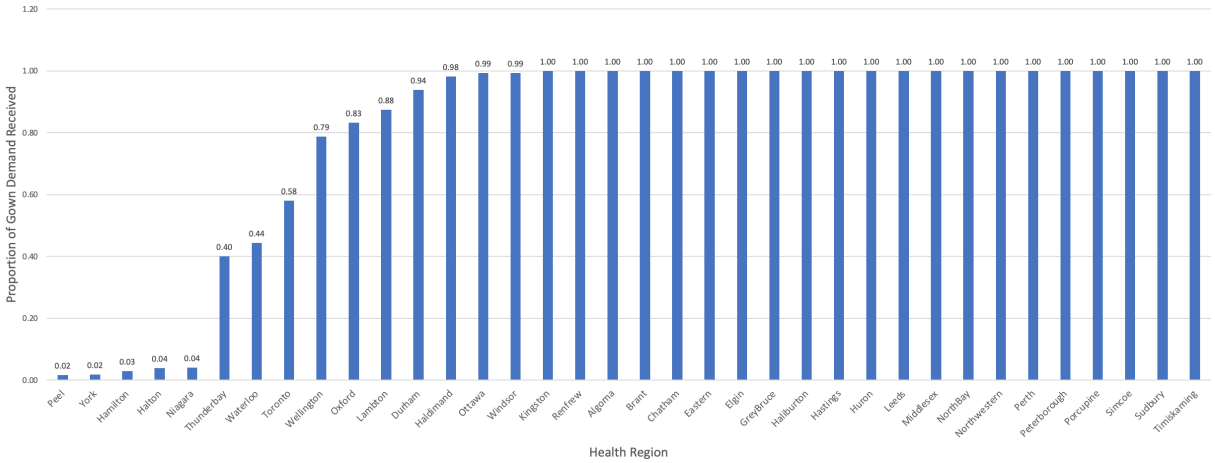

Figure 5.10: Average Proportion of Gown Demand Received Across all Time Periods

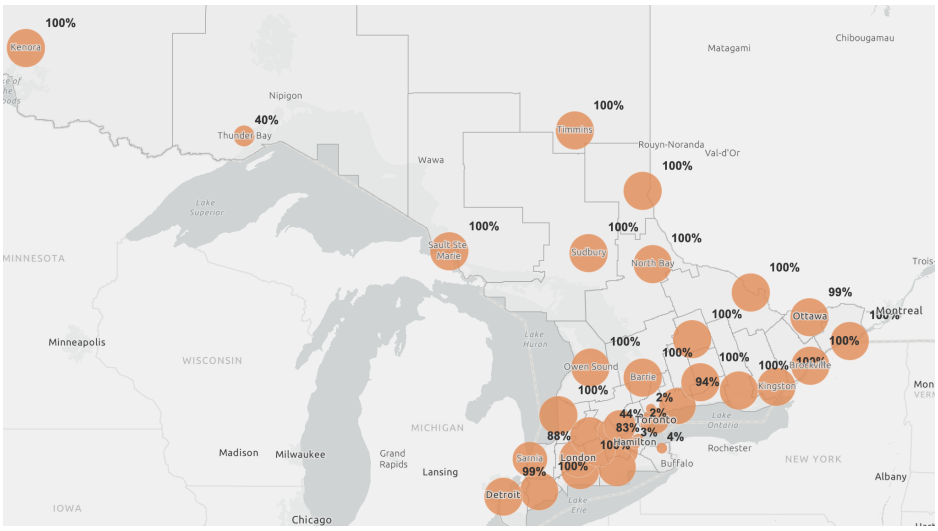

Figure 5.11: Map of Average Proportion of Gown Demand Received Across all Time Periods

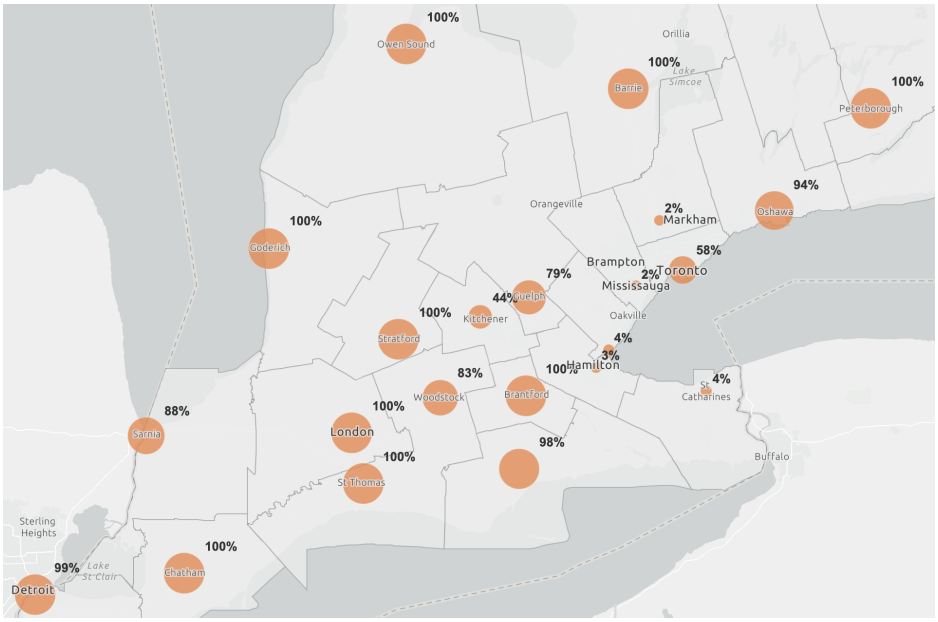

Figure 5.12: Map of Average Proportion of Gown Demand Received Across all Time Periods in Southern Ontario

In order to encourage high-priority regions to receive larger proportions of their demand, we normalize the priority values between ranges with larger upper bounds. Increasing the upper bound of the priority range as well as increasing the length of the priority value range will place a greater emphasis on supplying PPE to high-priority regions. Larger priority values will increase the denominator in the third term of the priority model objective function (3.10). By normalizing the priority values into such ranges, we would expect high-priority regions to receive larger proportions of their demand than low-priority regions. However, with priorities normalized in the range 1-100,000, results were very similar to the solution obtained using the original priority values. Table 5.6 compares the proportions of demand received in the regions with the largest priority values: Toronto, York, and Peel. The increased priority values does not make a large impact on the mask demand. For gown demand, the increased priority values increase the York and Peel proportions to 20% and 17%, respectively. Toronto, however, actually receives a lower proportion of its gown demand given the higher priority values.

Table 5.6: Proportion of Demand Received for Toronto, York, and Peel with the Original Insufficient Supply Data

Health Region	**Product**	**Proportion of Demand Received with Original Priority Values**	**Proportion of Demand Received with Priority Values Between 1-100,000**
Toronto	**Mask**	0.60	0.60
	Gown	0.58	0.28
York	**Mask**	0.97	1.00
	Gown	0.02	0.20
Peel	**Mask**	1.00	0.98
	Gown	0.02	0.17

For comparison, we tested the priority model with supply spread more evenly between the health regions, as shown in Table 5.7. Table 5.8 presents the proportions of demand received in Toronto, York, and Peel for the original and normalized priority values given

the new supply data. With supply spread more evenly around the province, each of the three large health regions receive at least 22% of their demand for each product. Having supply spread out throughout the province encourages a more even distribution of PPE than when supply is concentrated at a few locations. Similarly to previous test cases, larger priority values do not significantly impact the proportion of demand received at high-priority regions.

5.3 Supply Disturbances

We consider a disturbance in the available PPE supply where there is no supply in the network during the third time period. Supply during the other three time periods remains the same. When running this test case, we found that $21,000$ PPE units of warehouse capacity were acquired in Ottawa. As Table 5.9 shows, the model incrementally built up the amount of inventory at the Ottawa warehouse, which is used to supply the entire province during the third time period. All acquired warehouse capacity is used after the second time period. Since the Ottawa warehouse capacity cannot store enough inventory to satisfy all demand in the province, on average only 9.7% of demand is satisfied during the third time period.

5.4 Increased Route Capacity

We consider two settings in which larger route capacities are available. We define Setting A to be the test case with the original route capacity values. For Setting B, we consider the available route capacity for Carrier B to be double the destination demand for each route. For example, the District of Algoma Health Region requires a total of $6,265$ units of

Table 5.7: Supply per Time Period Spread Throughout the Network

Product	Mask Supply	Gown Supply
Algoma	300	21,500
Brant	300	700
Chatham-Kent	300	700
Durham	300	700
Eastern	300	700
Elgin	300	700
Grey Bruce	300	700
Haldimand	300	700
Haliburton	300	700
Halton	300	700
Hamilton	9,300	21,500
Hastings	300	700
Huron	300	700
Kingston	300	700
Lambton	300	700
Leeds	300	700
Middlesex	300	700
Niagara	300	700
North Bay	300	700
Northwestern	300	700
Ottawa	30,400	76,200
Oxford	300	700
Peel	9,300	41,500
Perth	300	700
Peterborough	300	700
Porcupine	300	700
Renfrew	300	700
Simcoe	300	700
Sudbury	9,300	21,500
Thunder Bay	9,300	700
Timiskaming	300	700
Toronto	20,200	35,800
Waterloo	300	700
Wellington	300	700
Windsor	26,100	12,500
York	300	700
Total	**122,600**	**250,800**

Table 5.8: Proportion of Demand Received for Toronto, York, and Peel with the More Evenly Spread Supply Data

Health Region	**Product**	**Proportion of Demand Received with Original Priority Values**	**Proportion of Demand Received with Priority Values Between 1-100,000**
Toronto	Mask	0.30	0.30
	Gown	0.22	0.22
York	Mask	0.82	0.82
	Gown	0.58	0.58
Peel	Mask	0.44	0.44
	Gown	0.82	0.82

Table 5.9: Inventory Stored at Ottawa Warehouse

Time Period	**Amount of Mask Inventory in Ottawa Warehouse**	**Amount of Gown Inventory in Ottawa Warehouse**
1	5,240	5,261
2	10,477	10,523
3	0	0
4	2,134	7,488

demand per time period. Thus, $h^r_{i,j} = 12,530 \ \forall i$, where $j = Algoma$, $r = Carrier\ B$. The Carrier A route capacities remain unchanged. Setting C considers the available capacity for both carriers to be double the destination demand for each route. Table 5.10 compares the total route capacity acquired from each carrier as well as the recourse objective value for each setting.

5.4.1 Increased Carrier B Capacity

For Setting B, only Carrier B has double the available route capacity and Benders decomposition solves to a gap of 0.08% in about 22 minutes. From Table 5.10, we see that the total capacity acquired from Carrier A increases while the total capacity acquired from Carrier B decreases. Since the increased Carrier B route capacity also increases the cost to acquire route the capacity, Carrier A capacity will be acquired where possible. We also notice that the recourse objective value decreases with this increased capacity. This is due to larger route capacities allowing for more direct rerouting of PPE.

5.4.2 Increased Capacity for Both Carriers

For Setting C, all routes for both carriers have double the available capacity and the Benders decomposition algorithm solves to an optimality gap of 0.23% in about 24 minutes. Table 5.10 shows that the capacity acquisition decisions no longer favour Carrier A. Since the route acquisition costs for each carrier are identical, Carrier B capacity is acquired by default and Carrier A capacity is only acquired when there is not enough from Carrier B. The Setting C recourse objective value is also smaller than the Setting A recourse function value. This indicates that savings are achieved from economies of scale by distributing PPE in larger shipments. The recourse value for Setting C is greater that for Setting B as

Setting B allows for either large or small route capacities to be acquired. The government is not forced to acquire large route capacities in all cases.

Table 5.10: Change in Route Capacity Acquired Under Different Capacity Settings

Setting	Total Carrier A Route Capacity Acquired	Total Carrier B Route Capacity Acquired	Recourse Objective Value
Setting A: Initial Capacities	515,198	1,057,156	12,653
Setting B: Increased Capacities for Carrier B Only	831,598	636,702	3,377
Setting C: Increased Capacities for Both Carriers	221,086	1,854,910	9,656

Chapter 6

Conclusion

In this thesis, we studied the problem of distributing PPE during the COVID-19 pandemic by acquiring route and storage capacity from independent carriers. We presented a deterministic model which prioritized distribution based on pandemic risk level in the event of insufficient supply. In addition, we proposed a two-stage stochastic model with recourse for PPE distribution under uncertain demand.

The stochastic model was approximated using sample average approximation and solved using Benders decomposition on test cases of Ontario health units and with $1,024$ scenarios. Both algorithms had an optimality gap of less than 0.31%. Benders decomposition solved for all $1,024$ scenarios in approximately 20 minutes, while sample average approximation solved using $M = 20$ samples each of size $N = 20$ in approximately one hour. When comparing the stochastic model solution with the actual demand values once they became known, the stochastic model is able to satisfy demand at all locations. The net PPE received at each location was greater than the location's demand. Only the minimum amount of necessary supply is rerouted in the second stage to satisfy demand increases, which are often met from stored inventory.

Regardless of whether supply was concentrated at a few locations or spread throughout the network, the priority values in the priority model did not have a large impact on distribution. However, a larger range for priority values did increase the amount of demand received for locations that receive very small proportions of demand. If supply is more spread out throughout the network, the proportion of demand received at each location is more balanced and high priority regions received at least 22% of their demand. In the event of supply disturbances, warehouse capacity is acquired to stockpile demand for time periods without supply. Having multiple options for sizes of route capacities decreases the required rerouting costs.

Potential future research based on the priority model could explore adjusting the priority in between time periods to reflect the amount of PPE received during the previous time period. For example, a location which does not receive very much PPE during a time period could have its priority increased for the next time period. Future work regarding the stochastic model could explore uncertainty in supply or expand the stochastic model to be multi-stage.

References

D. Alem, A. Clark, and A. Moreno. Stochastic network models for logistics planning in disaster relief. *European Journal of Operational Research*, 255(1):187–206, 2016. ISSN 0377-2217. doi: https://doi.org/10.1016/j.ejor.2016.04.041. URL https://www.sciencedirect.com/science/article/pii/S0377221716302788.

K. Alicke, X. Azcue, and E. Barriball. Supply-chain recovery in coronavirus times—plan for now and the future, 2020. URL https://www.mckinsey.com/~/media/McKinsey/Business%20Functions/Operations/Our%20Insights/Supply%20chain%20recovery%20in%20coronavirus%20times%20plan%20for%20now%20and%20the%20future/Supply-chain-recovery-in-coronavirus-times-plan-for-now-and-the-future.pdf.

M. Amini and H. Li. Supply chain configuration for diffusion of new products: An integrated optimization approach. *Omega*, 39(3):313–322, 2011. ISSN 0305-0483. doi: https://doi.org/10.1016/j.omega.2010.07.009. URL https://www.sciencedirect.com/science/article/pii/S0305048310000988.

R. Bai, S. W. Wallace, J. Li, and A. Y.-L. Chong. Stochastic service network design with rerouting. *Transportation Research Part B: Methodological*, 60:50–65, 2014.

ISSN 0191-2615. doi: https://doi.org/10.1016/j.trb.2013.11.001. URL https://www.sciencedirect.com/science/article/pii/S0191261513001999.

G. Barbarosoğlu and Y. Arda. A two-stage stochastic programming framework for transportation planning in disaster response. *Journal of the Operational Research Society*, 55 (1):43–53, 2004. doi: 10.1057/palgrave.jors.2601652. URL https://doi.org/10.1057/palgrave.jors.2601652.

M. Brandenburg. Low carbon supply chain configuration for a new product – a goal programming approach. *International Journal of Production Research*, 53(21):6588–6610, November 2015. doi: 10.1080/00207543.2015.100. URL https://ideas.repec.org/a/taf/tprsxx/v53y2015i21p6588-6610.html.

Canadian Institute for Health Information. Hospital beds staffed and in operation, 2018-2019, 2020. URL https://www.cihi.ca/en/search?query=hospital+beds&Search+Submit=.

L. Castro, S. Fox, X. Chen, K. Liu, S. Bellan, N. Dimitrov, A. Galvani, and L. Meyers. Assessing real-time zika risk in the united states. *BMC Infectious Diseases*, 17, 05 2017. doi: 10.1186/s12879-017-2394-9.

Cerasis Inc. Trailer guide, 2015. URL https://cerasis.com/wp-content/uploads/2015/08/2015TrailerGuide.pdf.

S. S. Chauhan, R. Nagi, and J.-M. Proth. Strategic capacity planning in supply chain design for a new market opportunity. *International Journal of Production Research*, 42 (11):2197–2206, 2004. doi: 10.1080/0020754042000197711. URL https://doi.org/10.1080/0020754042000197711.

S. S. Chauhan, J.-M. Proth, A. M. Sarmiento, and R. Nagi. Opportunistic supply chain formation from qualified partners for a new market demand. *Journal of the Operational Research Society*, 57(9):1089–1099, 2006. doi: 10.1057/palgrave.jors.2602075. URL https://doi.org/10.1057/palgrave.jors.2602075.

J. Chiu. Please use hand sanitizer! retail workers, customers navigate new normal as covid-19 lockdown eases., 2020. URL https://www.thestar.com/news/canada/2020/06/05/please-use-hand-sanitizer-retail-workers-customers-navigate-new-normal-as-covid-19-l html.

E. Chung. Mandatory mask laws are spreading in canada, 2020. URL https://www.cbc.ca/news/health/mandatory-masks-1.5615728.

S. Collis and D. Ungerman. Safeguarding the lifeblood of american healthcare: An interview with the ceo of amrisourcebergen., August 2020. URL https://www.mckinsey.com/industries/healthcare-systems-and-services/our-insights/safeguarding-the-lifeblood-of-american-healthcare-an-interview-with-the-ceo-of-ameri

A. Cozzolino, E. Wankowicz, and E. Massaroni. Logistics service providers' engagement in disaster relief initiatives: An exploratory analysis. *International Journal of Quality and Service Sciences*, 9:269–291, 2017. ISSN 1756-669X. doi: 10.1108/IJQSS-04-2017-0040.

A. Döyen, N. Aras, and G. Barbarosoglu. A two-echelon stochastic facility location model for humanitarian relief logistics. *Optimization Letters*, 6(6):1123–1145, August 2012. doi: 10.1007/s11590-011-0421-0.

E. Dyer. The great ppe panic: How the pandemic caught canada with its stockpiles down., 2020. URL https://www.cbc.ca/news/politics/ppe-pandemic-covid-coronavirus-masks-1.5645120.

Fedex Canada. Calculate shipping rates, 2021. URL https://www.fedex.com/en-ca/online/rating.html.

Jane Feinmann. Ppe: what now for the global supply chain? *BMJ*, 369, 2020. doi: 10.1136/bmj.m1910. URL https://www.bmj.com/content/369/bmj.m1910.

R. Flanagan. With some provinces reopening, where does canada's ppe supply chain stand?, 2020. URL https://www.ctvnews.ca/health/coronavirus/with-some-provinces-reopening-where-does-canada-s-ppe-supply-chain-stand-1.4922887.

Freight Quote by C.H. Robinson. Standard pallet sizes, 2020. URL https://www.freightquote.com/how-to-ship-freight/standard-pallet-sizes/.

L. Geng, R. Xiao, and J. Chen. Resilience design of healthcare resources supply network based on self-organized criticality. *Healthcare*, 8(3), 2020. ISSN 2227-9032. doi: 10.3390/healthcare8030245. URL https://www.mdpi.com/2227-9032/8/3/245.

Google Maps, 2021. URL https://www.google.com/maps.

Government of Canada. Government of canada awards contract to distribute covid-19 vaccine from coast to coast to coast, December 2020a. URL https://www.canada.ca/en/public-services-procurement/news/2020/12/government-of-canada-awards-contract-to-distribute-covid-19-vaccine-from-coast-to-co
html.

Government of Canada. Organizations buying and selling personal protective equipment during covid-19: Overview., 2020b. URL https://www.canada.ca/en/public-services-procurement/services/buying-selling-personal-protective-equipment-covid-19-overview.html.

Greater New York Hospital Association. Weekly ppe deliveries and ongoing supply results, 2020. URL https://www.gnyha.org/news/weekly-ppe-deliveries-and-ongoing-supply-requests/.

B. Hill. Coronavirus: Canada's supply of ppe won't meet demand as economy reopens, trade expert says, 2020. URL https://globalnews.ca/news/7024942/canada-ppe-supply-demand-coronavirus-reopening/.

R. Hoek. Research opportunities for a more resilient post-covid-19 supply chain – closing the gap between research findings and industry practice. *International Journal of Operations & Production Management*, ahead-of-print:341–355, 06 2020. doi: 10.1108/IJOPM-03-2020-0165.

A. Hooper and D. Murray. An analysis of the operational costs of trucking: 2018 update. *American Transport Research Institute*, 2018. URL https://truckingresearch.org/wp-content/uploads/2018/10/ATRI-Operational-Costs-of-Trucking-2018.pdf.

R. Hoppe. Chapter 1 stochastic linear and nonlinear programming, 2007.

D. Ivanov and A. Dolgui. Viability of intertwined supply networks: extending the supply chain resilience angles towards survivability. a position paper motivated by covid-19 outbreak. *International Journal of Production Research*, 58(10):2904–2915, 2020. doi: 10.1080/00207543.2020.1750727. URL https://doi.org/10.1080/00207543.2020.1750727.

M. Jahre and L.-M. Jensen. Coordination in humanitarian logistics through clusters. *International Journal of Physical Distribution & Logistics Management*, 40:657–674, 09 2010. doi: 10.1108/09600031011079319.

E. Javan, S.J. Fox, and L.A. Meyers. Probability of current covid-19 outbreaks in all us counties. *The University of Texas at Austin*, 2020.

D. Kasilingam, S. P. Sathiya Prabhakaran, D. K. Rajendran, V. Rajagopal, T. Santhosh Kumar, and A. Soundararaj. Exploring the growth of covid-19 cases using exponential modelling across 42 countries and predicting signs of early containment using machine learning. *Transboundary and emerging diseases*, 68(3):1001—1018, May 2021. ISSN 1865-1674. doi: 10.1111/tbed.13764.

M.H. Kutner, C. Nachtsheim, J. Neter, and W. Li. *Applied Linear Statistical Models*. McGraw-Hill Irwin, 5th ed. edition, 2005.

Scott Laing and Ellen Westervelt. Canada's national emergency stockpile system: time for a new long-term strategy. *CMAJ*, 192(28):E810–E811, 2020. ISSN 0820-3946. doi: 10.1503/cmaj.200946. URL https://www.cmaj.ca/content/192/28/E810.

J. Luedtke. Benders decomposition for solving two-stage stochastic optimization models, August 2016. URL https://www.ima.umn.edu/Tags/Stochastic-programming.

J. M. Martin-Olalla. Exponential distribution of large excess death rates in europe during the covid-19 outbreak in the spring of 2020. *medRxiv*, 2020. doi: 10.1101/2020.09.20.20198283.

H. O. Mete and Z. B. Zabinsky. Stochastic optimization of medical supply location and distribution in disaster management. *International Journal of Production Economics*, 126 (1):76–84, 2010. ISSN 0925-5273. doi: https://doi.org/10.1016/j.ijpe.2009.10.004. URL https://www.sciencedirect.com/science/article/pii/S0925527309003582. Improving Disaster Supply Chain Management – Key supply chain factors for humanitarian relief.

Ministry of Education. Covid-19: health and safety measures at schools, July 2021. URL https://www.ontario.ca/page/covid-19-health-and-safety-measures-schools.

Ministry of Government and Consumer Services. Supply ontario, 2021. URL https://www.ontario.ca/page/supply-ontario.

Ministry of Health. Face coverings and face masks, May 2021. URL https://www.ontario.ca/page/face-coverings-and-face-masks.

L.H. Nguyen, D.A. Drew, M.S. Graham, A.D. Joshi, C.-G. Guo, W. Ma, R.S. Mehta, E.T. Warner, D.R. Sikavi, C.-H. Lo, S. Kwon, M. Song, L.A. Mucci, M.J. Stampfer, W.C. Willett, A.H. Eliassen, J.E. Hart, J.E. Chavarro, J.W. Rich-Edwards, R. Davies, J. Capdevilla, K.A. Lee, M. N. Lochlainn, T. Varsavsky, C.H. Sudre, M.J. Cardoso, J. Wolf, T.D. Spector, S. Ourselin, C.J. Steves, and A.T. Chan. Risk of covid-19 among front-line health-care workers and the general community: a prospective cohort study. *Lancet Public Health 2020*, 5(9), September 2020. doi: 10.1016/S2468-2667(20)30164-X. URL https://www.thelancet.com/journals/lanpub/article/PIIS2468-2667(20)30164-X/fulltext.

V. I. Norkin, G.C. Pflug, and A. Ruszczyński. A branch and bound method for stochastic global optimization. *Mathematical Programming*, pages 425–450, January 1998. doi: https://doi.org/10.1007/BF02680569.

North American Rescue. Disposable surgical masks - level 2 (box of 50), 2020. URL https://www.narescue.com/disposable-face-masks-box-of-50.html.

Ontario.ca. Covid-19 response framework: keeping ontario safe and open, 2020a. URL https://www.ontario.ca/page/covid-19-response-framework-keeping-ontario-safe-and-open#control.

Ontario.ca. Covid-19 case data: All ontario, 2020b. URL https://covid-19.ontario.ca/data.

O. Y. Özaltın, O. A. Prokopyev, and A. J. Schaefer. Optimal design of the seasonal influenza vaccine with manufacturing autonomy. *INFORMS J. on Computing*, 30(2): 371–387, May 2018. ISSN 1526-5528. doi: 10.1287/ijoc.2017.0786. URL https://doi.org/10.1287/ijoc.2017.0786.

F. Pan and R. Nagi. Robust supply chain design under uncertain demand in agile manufacturing. *Computers & Operations Research*, 37(4):668–683, 2010. ISSN 0305-0548. doi: https://doi.org/10.1016/j.cor.2009.06.017. URL https://www.sciencedirect.com/science/article/pii/S0305054809001683.

C.-Y. Park, K. Kim, S. Roth, S. Beck, J. W. Kang, M. C. Tayag, and Griffin M. Global shortage of personal proective equipment amid covid-19: Supply chains, bottlenecks, and policy implications. *Asian Development Bank*, April 2020. ISSN 2218-2675. doi: http://dx.doi.org/10.22617/BRF200128-2.

A. Patel, M. D'Alessandro, K. Ireland, W. Burel, E. Wencil, and S. Rasmussen. Personal protective equipment supply chain: Lessons learned from recent public health emergency responses. *Health Security*, 15:244–252, 06 2017. doi: 10.1089/hs.2016.0129.

S. Pettit and Anthony Beresford. Critical success factors in the context of humanitarian aid supply chains. *International Journal of Physical Distribution & Logistics Management*, 39:450–468, 07 2009. doi: 10.1108/09600030910985811.

D. Polygenis. Is canada's supply chain ready for a covid-19 vaccine?, September 2020. URL https://www.mckesson.ca/documents/59196/0/McKesson+

Canada+Whitepaper+-+COVID-19+Vaccine+Supply+Chain+Readiness.pdf/e2e85307-662f-0ffe-0a60-7cf120802cd6.

Public Health Ontario. Considerations for community-based health care workers on interpreting local epidemiology, 2020. URL https://www.publichealthontario.ca/-/media/documents/ncov/ipac/2020/09/community-based-health-care-workers-interpreting-local-epi.pdf?la=en.

Quebec.ca. Universal mask use in health care settings and retirement homes, 2021. URL https://www.publichealthontario.ca/-/media/documents/ncov/ipac/report-covid-19-universal-mask-use-health-care-settings.pdf?la=en.

J. Rocklöv and H. Sjödin. High population densities catalyse the spread of COVID-19. *Journal of Travel Medicine*, 27(3), 03 2020. ISSN 1708-8305. doi: 10.1093/jtm/taaa038. URL https://doi.org/10.1093/jtm/taaa038. taaa038.

N. J. Rowan and J. G. Laffey. Challenges and solutions for addressing critical shortage of supply chain for personal and protective equipment (ppe) arising from coronavirus disease (covid19) pandemic – case study from the republic of ireland. *Science of The Total Environment*, 725:138532, 2020. ISSN 0048-9697. doi: https://doi.org/10.1016/j.scitotenv.2020.138532. URL https://www.sciencedirect.com/science/article/pii/S0048969720320453.

Statista. Canada: Inflation rate from 1986 to 2026, 2021. URL https://www.statista.com/statistics/271247/inflation-rate-in-canada/.

Statistics Canada. Census profile, 2016 census, 2020. URL https://www12.statcan.gc.ca/census-recensement/2016/dp-pd/prof/index.cfm?Lang=E.

A. Tabah, M. Ramanan, K. B. Laupland, N. Buetti, A. Cortegiani, J. Mellinghoff, A. Conway Morris, L. Camporota, N. Zappella, M. Elhadi, P. Povoa, K. Amrein, G. Vidal, L. Derde, M. Bassetti, G. Francois, N. Ssi yan kai, and J. J. De Waele. Personal protective equipment and intensive care unit healthcare worker safety in the covid-19 era (ppe-safe): An international survey. *Journal of Critical Care*, 59:70–75, 2020. ISSN 0883-9441. doi: https://doi.org/10.1016/j.jcrc.2020.06.005. URL https://www.sciencedirect.com/science/article/pii/S088394412030592X.

The Canadian Press. Military, health officials doing a practice run of coronavirus vaccine rollout, 2020. URL https://www.ctvnews.ca/health/coronavirus/military-health-officials-doing-a-practice-run-of-coronavirus-vaccine-rollout-1.5220085.

R. M. Tomasini and L. N. Van Wassenhove. From preparedness to partnerships: case study research on humanitarian logistics. *International Transactions in Operational Research*, 16(5):549–559, 2009. doi: https://doi.org/10.1111/j.1475-3995.2009.00697.x. URL https://onlinelibrary.wiley.com/doi/abs/10.1111/j.1475-3995.2009.00697.x.

U.S. Food and Drug Administration. Personal protective equipment for infection control, 2020. URL https://www.fda.gov/medical-devices/general-hospital-devices-and-supplies/personal-protective-equipment-infection-control.

B. Verweij, S. Ahmed, A. J. Kleywegt, G. Nemhauser, and A. Shapiro. The sample average approximation method applied to stochastic routing problems: A computational study. *Computational Optimization and Applications*, 24(2-3):289, Feb 2003. URL http://search.proquest.com.proxy.lib.uwaterloo.ca/scholarly-journals/

sample-average-approximation-method-applied/docview/215644679/se-2?accountid=14906. Copyright - Copyright Kluwer Academic Publishers Feb/Mar 2003; Last updated - 2014-08-30.

M. Warren. Health-care workers at two toronto hospitals told they'll soon be reusing decontaminated n95 masks, 2020. URL https://www.thestar.com/news/gta/2020/04/10/health-care-workers-at-two-toronto-hospitals-told-theyll-soon-be-reusing-decontamina html.

M.K. Zanjani, M. Nourelfath, and D. Ait-Kadi. A multi-stage stochastic programming approach for production planning with uncertainty in the quality of raw materials and demand. *Interuniversity Research Centre on Enterprise Networks, Logistics and Transportation*, 2009.

APPENDICES

Appendix A

Tables

Table A.1: Road Distance Between Health Regions, Part 1

	Algoma	**Brant**	**Chatham**	**Durham**	**Eastern**	**Elgin**
Algoma	0	771	948	677	892	856
Brant	771	0	195	163	539	104
Chatham	948	195	0	339	715	110
Durham	677	163	339	0	380	251
Eastern	892	539	715	380	0	624
Elgin	856	104	110	251	624	0
GreyBruce	671	194	306	234	610	242
Haldimand	813	42	185	206	582	79
Haliburton	784	220	396	61	322	305
Halton	723	54	240	116	492	150
Hamilton	734	41	228	126	502	137
Hastings	854	290	466	131	257	375
Huron	776	167	175	271	647	129
Kingston	930	365	541	206	183	451
Lambton	945	192	76	337	713	115
Leeds	879	441	617	282	102	526
Middlesex	846	94	114	239	615	27
Niagara	777	106	284	170	546	193
NorthBay	436	429	602	305	458	515
Northwestern	1169	1933	2111	1841	2026	2020
Ottawa	793	552	677	393	103	599
Oxford	794	44	155	186	562	64
Peel	689	88	271	82	458	181
Perth	801	80	182	194	570	92
Peterborough	695	241	413	82	355	327
Porcupine	438	790	948	666	819	875
Renfrew	649	489	661	352	248	574
Simcoe	591	183	355	139	516	268
Sudbury	309	473	645	379	584	558
Thunderbay	705	1472	1647	1380	1563	1560
Timiskaming	617	671	846	547	700	756
Toronto	698	105	292	61	437	201
Waterloo	765	55	216	158	534	125
Wellington	745	50	220	138	514	129
Windsor	1023	271	82	416	792	187
York	657	121	297	68	444	206

Table A.2: Road Distance Between Health Regions, Part 2

	GreyBruce	**Haldimand**	**Haliburton**	**Halton**	**Hamilton**	**Hastings**
Algoma	671	813	784	723	734	854
Brant	194	42	220	54	41	290
Chatham	306	185	396	240	228	466
Durham	234	206	61	116	126	131
Eastern	610	582	322	492	502	257
Elgin	242	79	305	150	137	375
GreyBruce	0	225	291	205	186	361
Haldimand	225	0	262	96	83	332
Haliburton	291	262	0	173	184	75
Halton	205	96	173	0	19	242
Hamilton	186	83	184	19	0	253
Hastings	361	332	75	242	253	0
Huron	131	174	328	190	184	398
Kingston	436	408	150	317	329	83
Lambton	257	203	394	240	227	465
Leeds	512	483	226	393	405	158
Middlesex	204	104	296	142	128	366
Niagara	259	110	227	55	55	298
NorthBay	352	472	371	381	398	393
Northwestern	1835	1977	1949	1887	1900	2019
Ottawa	585	556	337	504	516	230
Oxford	179	60	243	93	79	314
Peel	167	130	139	40	52	210
Perth	150	98	251	114	107	321
Peterborough	312	283	57	193	205	106
Porcupine	676	832	732	742	739	754
Renfrew	463	531	296	441	453	227
Simcoe	118	225	197	135	146	267
Sudbury	372	515	447	425	436	557
Thunderbay	1371	1514	1485	1424	1437	1556
Timiskaming	594	713	613	623	634	635
Toronto	190	147	118	57	69	189
Waterloo	145	77	215	77	71	285
Wellington	135	94	195	53	47	265
Windsor	395	263	473	319	305	543
York	175	163	125	73	85	196

Table A.3: Road Distance Between Health Regions, Part 3

	Huron	**Kingston**	**Lambton**	**Leeds**	**Middlesex**	**Niagara**
Algoma	776	930	945	879	846	777
Brant	167	365	192	441	94	106
Chatham	175	541	76	617	114	284
Durham	271	206	337	282	239	170
Eastern	647	183	713	102	615	546
Elgin	129	451	115	526	27	193
GreyBruce	131	436	257	512	204	259
Haldimand	174	408	203	483	104	110
Haliburton	328	150	394	226	296	227
Halton	190	317	240	393	142	55
Hamilton	184	329	227	405	128	55
Hastings	398	83	465	158	366	298
Huron	0	471	126	547	100	239
Kingston	471	0	539	86	441	372
Lambton	126	539	0	615	101	282
Leeds	547	86	615	0	515	446
Middlesex	100	441	101	515	0	184
Niagara	239	372	282	446	184	0
NorthBay	451	448	603	443	505	436
Northwestern	1940	2016	2109	2011	2011	1942
Ottawa	620	197	726	114	590	521
Oxford	120	388	153	462	55	145
Peel	201	284	270	358	172	95
Perth	73	396	140	470	61	166
Peterborough	347	181	415	255	317	248
Porcupine	781	808	950	803	852	783
Renfrew	595	242	663	232	565	496
Simcoe	205	342	357	416	259	190
Sudbury	478	631	647	569	549	480
Thunderbay	1477	1553	1646	1548	1548	1479
Timiskaming	692	689	845	684	747	678
Toronto	225	263	290	337	192	112
Waterloo	113	360	214	434	116	130
Wellington	147	340	218	414	120	105
Windsor	266	618	156	692	191	371
York	227	270	295	344	197	128

Table A.4: Road Distance Between Health Regions, Part 4

	NorthBay	**Northwestern**	**Ottawa**	**Oxford**	**Peel**	**Perth**
Algoma	436	1169	793	794	689	801
Brant	429	1933	552	44	88	80
Chatham	602	2111	677	155	271	182
Durham	305	1841	393	186	82	194
Eastern	458	2026	103	562	458	570
Elgin	515	2020	599	64	181	92
GreyBruce	352	1835	585	179	167	150
Haldimand	472	1977	556	60	130	98
Haliburton	371	1949	337	243	139	251
Halton	381	1887	504	93	40	114
Hamilton	398	1900	516	79	52	107
Hastings	393	2019	230	314	210	321
Huron	451	1940	620	120	201	73
Kingston	448	2016	197	388	284	396
Lambton	603	2109	726	153	270	140
Leeds	443	2011	114	462	358	470
Middlesex	505	2011	590	55	172	61
Niagara	436	1942	521	145	95	166
NorthBay	0	1569	359	452	348	460
Northwestern	1569	0	1927	1957	1853	1965
Ottawa	359	1927	0	523	422	530
Oxford	452	1957	523	0	118	38
Peel	348	1853	422	118	0	127
Perth	460	1965	530	38	127	0
Peterborough	321	1858	271	261	159	267
Porcupine	362	1245	718	810	708	816
Renfrew	214	1783	147	509	407	515
Simcoe	249	1754	412	203	101	209
Sudbury	127	1472	483	493	391	499
Thunderbay	1106	489	1462	1492	1390	1498
Timiskaming	243	1348	598	691	589	697
Toronto	357	1862	411	143	28	149
Waterloo	424	1929	494	63	91	46
Wellington	404	1909	474	68	71	74
Windsor	682	2187	752	232	349	253
York	315	1820	392	141	40	148

Table A.5: Road Distance Between Health Regions, Part 5

	Peterborough	**Porcupine**	**Renfrew**	**Simcoe**	**Sudbury**	**Thunderbay**
Algoma	695	438	649	591	309	705
Brant	241	790	489	183	473	1472
Chatham	413	948	661	355	645	1647
Durham	82	666	352	139	379	1380
Eastern	355	819	248	516	584	1563
Elgin	327	875	574	268	558	1560
GreyBruce	312	676	463	118	372	1371
Haldimand	283	832	531	225	515	1514
Haliburton	57	732	296	197	447	1485
Halton	193	742	441	135	425	1424
Hamilton	205	739	453	146	436	1437
Hastings	106	754	227	267	557	1556
Huron	347	781	595	205	478	1477
Kingston	181	808	242	342	631	1553
Lambton	415	950	663	357	647	1646
Leeds	255	803	232	416	569	1548
Middlesex	317	852	565	259	549	1548
Niagara	248	783	496	190	480	1479
NorthBay	321	362	214	249	127	1106
Northwestern	1858	1245	1783	1754	1472	489
Ottawa	271	718	147	412	483	1462
Oxford	261	810	509	203	493	1492
Peel	159	708	407	101	391	1390
Perth	267	816	515	209	499	1498
Peterborough	0	681	246	201	396	1395
Porcupine	681	0	574	595	294	782
Renfrew	246	574	0	360	340	1319
Simcoe	201	595	360	0	292	1291
Sudbury	396	294	340	292	0	1007
Thunderbay	1395	782	1319	1291	1007	0
Timiskaming	562	140	455	490	308	879
Toronto	139	703	408	111	400	1393
Waterloo	231	766	479	174	463	1456
Wellington	211	746	459	154	443	1436
Windsor	489	1024	737	432	721	1714
York	129	661	377	69	358	1351

Table A.6: Road Distance Between Health Regions, Part 6

	Timiskaming	**Toronto**	**Waterloo**	**Wellington**	**Windsor**	**York**
Algoma	617	698	765	745	1023	657
Brant	671	105	55	50	271	121
Chatham	846	292	216	220	82	297
Durham	547	61	158	138	416	68
Eastern	700	437	534	514	792	444
Elgin	756	201	125	129	187	206
GreyBruce	594	190	145	135	395	175
Haldimand	713	147	77	94	263	163
Haliburton	613	118	215	195	473	125
Halton	623	57	77	53	319	73
Hamilton	634	69	71	47	305	85
Hastings	635	189	285	265	543	196
Huron	692	225	113	147	266	227
Kingston	689	263	360	340	618	270
Lambton	845	290	214	218	156	295
Leeds	684	337	434	414	692	344
Middlesex	747	192	116	120	191	197
Niagara	678	112	130	105	371	128
NorthBay	243	357	424	404	682	315
Northwestern	1348	1862	1929	1909	2187	1820
Ottawa	598	411	494	474	752	392
Oxford	691	143	63	68	232	141
Peel	589	28	91	71	349	40
Perth	697	149	46	74	253	148
Peterborough	562	139	231	211	489	129
Porcupine	140	703	766	746	1024	661
Renfrew	455	408	479	459	737	377
Simcoe	490	111	174	154	432	69
Sudbury	308	400	463	443	721	358
Thunderbay	879	1393	1456	1436	1714	1351
Timiskaming	0	598	662	641	920	557
Toronto	598	0	113	93	369	42
Waterloo	662	113	0	28	291	111
Wellington	641	93	28	0	297	94
Windsor	920	369	291	297	0	371
York	557	42	111	94	371	0

Table A.7: Unit Cost to Acquire Route Capacity Between Health Regions, Part 1

	Algoma	**Brant**	**Chatham**	**Durham**	**Eastern**	**Elgin**
Algoma	0.000	0.043	0.053	0.038	0.050	0.048
Brant	0.043	0.000	0.011	0.009	0.030	0.006
Chatham	0.053	0.011	0.000	0.019	0.040	0.006
Durham	0.038	0.009	0.019	0.000	0.021	0.014
Eastern	0.050	0.030	0.040	0.021	0.000	0.035
Elgin	0.048	0.006	0.006	0.014	0.035	0.000
GreyBruce	0.038	0.011	0.017	0.013	0.034	0.014
Haldimand	0.046	0.002	0.010	0.012	0.033	0.004
Haliburton	0.044	0.012	0.022	0.003	0.018	0.017
Halton	0.041	0.003	0.013	0.007	0.028	0.008
Hamilton	0.041	0.002	0.013	0.007	0.028	0.008
Hastings	0.048	0.016	0.026	0.007	0.014	0.021
Huron	0.044	0.009	0.010	0.015	0.036	0.007
Kingston	0.052	0.021	0.030	0.012	0.010	0.025
Lambton	0.053	0.011	0.004	0.019	0.040	0.006
Leeds	0.049	0.025	0.035	0.016	0.006	0.030
Middlesex	0.048	0.005	0.006	0.013	0.035	0.002
Niagara	0.044	0.006	0.016	0.010	0.031	0.011
NorthBay	0.025	0.024	0.034	0.017	0.026	0.029
Northwestern	0.066	0.109	0.119	0.103	0.114	0.114
Ottawa	0.045	0.031	0.038	0.022	0.006	0.034
Oxford	0.045	0.002	0.009	0.010	0.032	0.004
Peel	0.039	0.005	0.015	0.005	0.026	0.010
Perth	0.045	0.004	0.010	0.011	0.032	0.005
Peterborough	0.039	0.014	0.023	0.005	0.020	0.018
Porcupine	0.025	0.044	0.053	0.037	0.046	0.049
Renfrew	0.036	0.027	0.037	0.020	0.014	0.032
Simcoe	0.033	0.010	0.020	0.008	0.029	0.015
Sudbury	0.017	0.027	0.036	0.021	0.033	0.031
Thunderbay	0.040	0.083	0.093	0.078	0.088	0.088
Timiskaming	0.035	0.038	0.048	0.031	0.039	0.042
Toronto	0.039	0.006	0.016	0.003	0.025	0.011
Waterloo	0.043	0.003	0.012	0.009	0.030	0.007
Wellington	0.042	0.003	0.012	0.008	0.029	0.007
Windsor	0.057	0.015	0.005	0.023	0.045	0.011
York	0.037	0.007	0.017	0.004	0.025	0.012

Table A.8: Unit Cost to Acquire Route Capacity Between Health Regions, Part 2

	GreyBruce	**Haldimand**	**Haliburton**	**Halton**	**Hamilton**	**Hastings**
Algoma	0.038	0.046	0.044	0.041	0.041	0.048
Brant	0.011	0.002	0.012	0.003	0.002	0.016
Chatham	0.017	0.010	0.022	0.013	0.013	0.026
Durham	0.013	0.012	0.003	0.007	0.007	0.007
Eastern	0.034	0.033	0.018	0.028	0.028	0.014
Elgin	0.014	0.004	0.017	0.008	0.008	0.021
GreyBruce	0.000	0.013	0.016	0.012	0.010	0.020
Haldimand	0.013	0.000	0.015	0.005	0.005	0.019
Haliburton	0.016	0.015	0.000	0.010	0.010	0.004
Halton	0.012	0.005	0.010	0.000	0.001	0.014
Hamilton	0.010	0.005	0.010	0.001	0.000	0.014
Hastings	0.020	0.019	0.004	0.014	0.014	0.000
Huron	0.007	0.010	0.018	0.011	0.010	0.022
Kingston	0.025	0.023	0.008	0.018	0.018	0.005
Lambton	0.014	0.011	0.022	0.013	0.013	0.026
Leeds	0.029	0.027	0.013	0.022	0.023	0.009
Middlesex	0.011	0.006	0.017	0.008	0.007	0.021
Niagara	0.015	0.006	0.013	0.003	0.003	0.017
NorthBay	0.020	0.027	0.021	0.021	0.022	0.022
Northwestern	0.103	0.111	0.110	0.106	0.107	0.113
Ottawa	0.033	0.031	0.019	0.028	0.029	0.013
Oxford	0.010	0.003	0.014	0.005	0.004	0.018
Peel	0.009	0.007	0.008	0.002	0.003	0.012
Perth	0.008	0.006	0.014	0.006	0.006	0.018
Peterborough	0.018	0.016	0.003	0.011	0.012	0.006
Porcupine	0.038	0.047	0.041	0.042	0.042	0.042
Renfrew	0.026	0.030	0.017	0.025	0.025	0.013
Simcoe	0.007	0.013	0.011	0.008	0.008	0.015
Sudbury	0.021	0.029	0.025	0.024	0.025	0.031
Thunderbay	0.077	0.085	0.083	0.080	0.081	0.087
Timiskaming	0.033	0.040	0.034	0.035	0.036	0.036
Toronto	0.011	0.008	0.007	0.003	0.004	0.011
Waterloo	0.008	0.004	0.012	0.004	0.004	0.016
Wellington	0.008	0.005	0.011	0.003	0.003	0.015
Windsor	0.022	0.015	0.027	0.018	0.017	0.031
York	0.010	0.009	0.007	0.004	0.005	0.011

Table A.9: Unit Cost to Acquire Route Capacity Between Health Regions, Part 3

	Huron	**Kingston**	**Lambton**	**Leeds**	**Middlesex**	**Niagara**
Algoma	0.044	0.052	0.053	0.049	0.048	0.044
Brant	0.009	0.021	0.011	0.025	0.005	0.006
Chatham	0.010	0.030	0.004	0.035	0.006	0.016
Durham	0.015	0.012	0.019	0.016	0.013	0.010
Eastern	0.036	0.010	0.040	0.006	0.035	0.031
Elgin	0.007	0.025	0.006	0.030	0.002	0.011
GreyBruce	0.007	0.025	0.014	0.029	0.011	0.015
Haldimand	0.010	0.023	0.011	0.027	0.006	0.006
Haliburton	0.018	0.008	0.022	0.013	0.017	0.013
Halton	0.011	0.018	0.013	0.022	0.008	0.003
Hamilton	0.010	0.018	0.013	0.023	0.007	0.003
Hastings	0.022	0.005	0.026	0.009	0.021	0.017
Huron	0.000	0.026	0.007	0.031	0.006	0.013
Kingston	0.026	0.000	0.030	0.005	0.025	0.021
Lambton	0.007	0.030	0.000	0.035	0.006	0.016
Leeds	0.031	0.005	0.035	0.000	0.029	0.025
Middlesex	0.006	0.025	0.006	0.029	0.000	0.010
Niagara	0.013	0.021	0.016	0.025	0.010	0.000
NorthBay	0.025	0.025	0.034	0.025	0.028	0.025
Northwestern	0.109	0.113	0.119	0.113	0.113	0.109
Ottawa	0.035	0.011	0.041	0.006	0.033	0.029
Oxford	0.007	0.022	0.009	0.026	0.003	0.008
Peel	0.011	0.016	0.015	0.020	0.010	0.005
Perth	0.004	0.022	0.008	0.026	0.003	0.009
Peterborough	0.020	0.010	0.023	0.014	0.018	0.014
Porcupine	0.044	0.045	0.053	0.045	0.048	0.044
Renfrew	0.033	0.014	0.037	0.013	0.032	0.028
Simcoe	0.012	0.019	0.020	0.023	0.015	0.011
Sudbury	0.027	0.035	0.036	0.032	0.031	0.027
Thunderbay	0.083	0.087	0.093	0.087	0.087	0.083
Timiskaming	0.039	0.039	0.047	0.038	0.042	0.038
Toronto	0.013	0.015	0.016	0.019	0.011	0.006
Waterloo	0.006	0.020	0.012	0.024	0.007	0.007
Wellington	0.008	0.019	0.012	0.023	0.007	0.006
Windsor	0.015	0.035	0.009	0.039	0.011	0.021
York	0.013	0.015	0.017	0.019	0.011	0.007

Table A.10: Unit Cost to Acquire Route Capacity Between Health Regions, Part 4

	NorthBay	**Northwestern**	**Ottawa**	**Oxford**	**Peel**	**Perth**
Algoma	0.025	0.066	0.045	0.045	0.039	0.045
Brant	0.024	0.109	0.031	0.002	0.005	0.004
Chatham	0.034	0.119	0.038	0.009	0.015	0.010
Durham	0.017	0.103	0.022	0.010	0.005	0.011
Eastern	0.026	0.114	0.006	0.032	0.026	0.032
Elgin	0.029	0.114	0.034	0.004	0.010	0.005
GreyBruce	0.020	0.103	0.033	0.010	0.009	0.008
Haldimand	0.027	0.111	0.031	0.003	0.007	0.006
Haliburton	0.021	0.110	0.019	0.014	0.008	0.014
Halton	0.021	0.106	0.028	0.005	0.002	0.006
Hamilton	0.022	0.107	0.029	0.004	0.003	0.006
Hastings	0.022	0.113	0.013	0.018	0.012	0.018
Huron	0.025	0.109	0.035	0.007	0.011	0.004
Kingston	0.025	0.113	0.011	0.022	0.016	0.022
Lambton	0.034	0.119	0.041	0.009	0.015	0.008
Leeds	0.025	0.113	0.006	0.026	0.020	0.026
Middlesex	0.028	0.113	0.033	0.003	0.010	0.003
Niagara	0.025	0.109	0.029	0.008	0.005	0.009
NorthBay	0.000	0.088	0.020	0.025	0.020	0.026
Northwestern	0.088	0.000	0.108	0.110	0.104	0.110
Ottawa	0.020	0.108	0.000	0.029	0.024	0.030
Oxford	0.025	0.110	0.029	0.000	0.007	0.002
Peel	0.020	0.104	0.024	0.007	0.000	0.007
Perth	0.026	0.110	0.030	0.002	0.007	0.000
Peterborough	0.018	0.104	0.015	0.015	0.009	0.015
Porcupine	0.020	0.070	0.040	0.046	0.040	0.046
Renfrew	0.012	0.100	0.008	0.029	0.023	0.029
Simcoe	0.014	0.099	0.023	0.011	0.006	0.012
Sudbury	0.007	0.083	0.027	0.028	0.022	0.028
Thunderbay	0.062	0.027	0.082	0.084	0.078	0.084
Timiskaming	0.014	0.076	0.034	0.039	0.033	0.039
Toronto	0.020	0.105	0.023	0.008	0.002	0.008
Waterloo	0.024	0.108	0.028	0.004	0.005	0.003
Wellington	0.023	0.107	0.027	0.004	0.004	0.004
Windsor	0.038	0.123	0.042	0.013	0.020	0.014
York	0.018	0.102	0.022	0.008	0.002	0.008

Table A.11: Unit Cost to Acquire Route Capacity Between Health Regions, Part 5

	Peterborough	**Porcupine**	**Renfrew**	**Simcoe**	**Sudbury**	**Thunderbay**
Algoma	0.039	0.025	0.036	0.033	0.017	0.040
Brant	0.014	0.044	0.027	0.010	0.027	0.083
Chatham	0.023	0.053	0.037	0.020	0.036	0.093
Durham	0.005	0.037	0.020	0.008	0.021	0.078
Eastern	0.020	0.046	0.014	0.029	0.033	0.088
Elgin	0.018	0.049	0.032	0.015	0.031	0.088
GreyBruce	0.018	0.038	0.026	0.007	0.021	0.077
Haldimand	0.016	0.047	0.030	0.013	0.029	0.085
Haliburton	0.003	0.041	0.017	0.011	0.025	0.083
Halton	0.011	0.042	0.025	0.008	0.024	0.080
Hamilton	0.012	0.042	0.025	0.008	0.025	0.081
Hastings	0.006	0.042	0.013	0.015	0.031	0.087
Huron	0.020	0.044	0.033	0.012	0.027	0.083
Kingston	0.010	0.045	0.014	0.019	0.035	0.087
Lambton	0.023	0.053	0.037	0.020	0.036	0.093
Leeds	0.014	0.045	0.013	0.023	0.032	0.087
Middlesex	0.018	0.048	0.032	0.015	0.031	0.087
Niagara	0.014	0.044	0.028	0.011	0.027	0.083
NorthBay	0.018	0.020	0.012	0.014	0.007	0.062
Northwestern	0.104	0.070	0.100	0.099	0.083	0.027
Ottawa	0.015	0.040	0.008	0.023	0.027	0.082
Oxford	0.015	0.046	0.029	0.011	0.028	0.084
Peel	0.009	0.040	0.023	0.006	0.022	0.078
Perth	0.015	0.046	0.029	0.012	0.028	0.084
Peterborough	0.000	0.038	0.014	0.011	0.022	0.078
Porcupine	0.038	0.000	0.032	0.033	0.017	0.044
Renfrew	0.014	0.032	0.000	0.020	0.019	0.074
Simcoe	0.011	0.033	0.020	0.000	0.016	0.073
Sudbury	0.022	0.017	0.019	0.016	0.000	0.057
Thunderbay	0.078	0.044	0.074	0.073	0.057	0.000
Timiskaming	0.032	0.008	0.026	0.028	0.017	0.049
Toronto	0.008	0.040	0.023	0.006	0.022	0.078
Waterloo	0.013	0.043	0.027	0.010	0.026	0.082
Wellington	0.012	0.042	0.026	0.009	0.025	0.081
Windsor	0.027	0.058	0.041	0.024	0.041	0.096
York	0.007	0.037	0.021	0.004	0.020	0.076

Table A.12: Unit Cost to Acquire Route Capacity Between Health Regions, Part 6

	Timiskaming	**Toronto**	**Waterloo**	**Wellington**	**Windsor**	**York**
Algoma	0.035	0.039	0.043	0.042	0.057	0.037
Brant	0.038	0.006	0.003	0.003	0.015	0.007
Chatham	0.048	0.016	0.012	0.012	0.005	0.017
Durham	0.031	0.003	0.009	0.008	0.023	0.004
Eastern	0.039	0.025	0.030	0.029	0.045	0.025
Elgin	0.042	0.011	0.007	0.007	0.011	0.012
GreyBruce	0.033	0.011	0.008	0.008	0.022	0.010
Haldimand	0.040	0.008	0.004	0.005	0.015	0.009
Haliburton	0.034	0.007	0.012	0.011	0.027	0.007
Halton	0.035	0.003	0.004	0.003	0.018	0.004
Hamilton	0.036	0.004	0.004	0.003	0.017	0.005
Hastings	0.036	0.011	0.016	0.015	0.031	0.011
Huron	0.039	0.013	0.006	0.008	0.015	0.013
Kingston	0.039	0.015	0.020	0.019	0.035	0.015
Lambton	0.047	0.016	0.012	0.012	0.009	0.017
Leeds	0.038	0.019	0.024	0.023	0.039	0.019
Middlesex	0.042	0.011	0.007	0.007	0.011	0.011
Niagara	0.038	0.006	0.007	0.006	0.021	0.007
NorthBay	0.014	0.020	0.024	0.023	0.038	0.018
Northwestern	0.076	0.105	0.108	0.107	0.123	0.102
Ottawa	0.034	0.023	0.028	0.027	0.042	0.022
Oxford	0.039	0.008	0.004	0.004	0.013	0.008
Peel	0.033	0.002	0.005	0.004	0.020	0.002
Perth	0.039	0.008	0.003	0.004	0.014	0.008
Peterborough	0.032	0.008	0.013	0.012	0.027	0.007
Porcupine	0.008	0.040	0.043	0.042	0.058	0.037
Renfrew	0.026	0.023	0.027	0.026	0.041	0.021
Simcoe	0.028	0.006	0.010	0.009	0.024	0.004
Sudbury	0.017	0.022	0.026	0.025	0.041	0.020
Thunderbay	0.049	0.078	0.082	0.081	0.096	0.076
Timiskaming	0.000	0.034	0.037	0.036	0.052	0.031
Toronto	0.034	0.000	0.006	0.005	0.021	0.002
Waterloo	0.037	0.006	0.000	0.002	0.016	0.006
Wellington	0.036	0.005	0.002	0.000	0.017	0.005
Windsor	0.052	0.021	0.016	0.017	0.000	0.021
York	0.031	0.002	0.006	0.005	0.021	0.000

Table A.13: Daily COVID-19 Cases by Ontario health Region, Part 1

Date	Algoma	Brant	Chatham	Durham	Eastern	GreyBruce
1-Oct-20	0	0	0	15	6	2
2-Oct-20	1	1	2	12	3	3
3-Oct-20	0	2	1	12	8	1
4-Oct-20	0	4	0	12	15	1
5-Oct-20	1	1	0	14	9	2
6-Oct-20	2	0	0	13	3	0
7-Oct-20	0	3	0	31	4	0
8-Oct-20	0	2	0	20	7	0
9-Oct-20	2	6	0	39	7	2
10-Oct-20	0	3	0	11	4	0
11-Oct-20	0	2	0	12	4	2
12-Oct-20	0	5	0	23	11	0
13-Oct-20	0	7	0	42	23	2
14-Oct-20	0	10	0	29	28	0
15-Oct-20	0	6	0	33	9	1
16-Oct-20	0	7	1	33	6	1
17-Oct-20	0	1	0	26	17	1
18-Oct-20	1	4	1	30	13	3
19-Oct-20	0	11	4	36	0	0
20-Oct-20	0	5	6	24	15	1
21-Oct-20	0	2	5	42	9	0
22-Oct-20	1	7	2	51	52	4
23-Oct-20	0	5	1	34	22	1
24-Oct-20	0	1	10	39	13	1
25-Oct-20	1	12	1	47	9	1
26-Oct-20	1	6	1	27	1	0
27-Oct-20	0	5	1	25	4	0
28-Oct-20	0	6	5	32	25	0
29-Oct-20	0	5	2	18	15	5
30-Oct-20	0	8	3	32	6	1
31-Oct-20	1	16	1	23	12	0
1-Nov-20	0	6	2	63	7	0
2-Nov-20	2	14	1	64	5	0
3-Nov-20	0	7	0	25	9	1
4-Nov-20	1	2	3	25	17	2
5-Nov-20	0	16	0	34	12	1
6-Nov-20	0	11	2	41	5	2
7-Nov-20	1	3	3	35	7	5
8-Nov-20	8	5	0	23	7	1
9-Nov-20	1	5	1	52	9	2

Table A.14: Daily COVID-19 Cases by Ontario health Region, Part 2

Date	Algoma	Brant	Chatham	Durham	Eastern	GreyBruce
10-Nov-20	1	3	14	58	3	0
11-Nov-20	0	3	1	32	8	7
12-Nov-20	0	3	13	61	12	7
13-Nov-20	0	10	3	41	4	2
14-Nov-20	0	11	1	64	5	5
15-Nov-20	0	4	4	62	5	5
16-Nov-20	1	9	7	45	9	10
17-Nov-20	0	9	6	69	5	2
18-Nov-20	0	3	3	40	2	2

Table A.15: Daily COVID-19 Cases by Ontario health Region, Part 3

Date	Haldimand	Haliburton	Halton	Hamilton	Hastings	Huron-Perth
1-Oct-20	0	1	12	7	1	0
2-Oct-20	1	0	29	12	2	0
3-Oct-20	1	1	17	5	1	3
4-Oct-20	0	1	24	13	0	0
5-Oct-20	2	1	20	21	0	1
6-Oct-20	0	1	34	19	0	0
7-Oct-20	2	0	26	22	0	1
8-Oct-20	0	0	56	24	0	1
9-Oct-20	1	0	43	53	2	0
10-Oct-20	2	0	34	31	1	2
11-Oct-20	1	1	20	21	0	2
12-Oct-20	0	0	32	25	0	0
13-Oct-20	1	0	28	30	1	0
14-Oct-20	0	0	44	21	0	0
15-Oct-20	2	0	19	14	1	1
16-Oct-20	1	0	41	15	1	1
17-Oct-20	1	0	26	20	1	0
18-Oct-20	1	1	34	35	0	0
19-Oct-20	1	0	33	19	0	1
20-Oct-20	1	0	20	25	3	0
21-Oct-20	1	0	30	17	2	0
22-Oct-20	2	1	29	14	1	1
23-Oct-20	4	2	22	14	2	0
24-Oct-20	9	0	37	36	1	1
25-Oct-20	6	0	19	21	0	0
26-Oct-20	3	1	17	20	0	0
27-Oct-20	2	0	38	22	1	0
28-Oct-20	2	0	22	17	0	3
29-Oct-20	2	2	42	30	1	2
30-Oct-20	2	1	23	37	1	5
31-Oct-20	1	1	22	35	1	2
1-Nov-20	1	0	49	31	0	1
2-Nov-20	1	0	59	30	0	0
3-Nov-20	4	1	48	27	0	1
4-Nov-20	4	1	43	42	2	6
5-Nov-20	3	2	49	53	1	6
6-Nov-20	5	0	52	49	0	4
7-Nov-20	6	1	54	55	0	5
8-Nov-20	3	1	53	56	0	9
9-Nov-20	1	1	45	39	0	17

Table A.16: Daily COVID-19 Cases by Ontario health Region, Part 4

Date	Haldimand	Haliburton	Halton	Hamilton	Hastings	Huron-Perth
10-Nov-20	2	0	44	42	0	8
11-Nov-20	0	0	21	16	0	4
12-Nov-20	3	0	54	30	0	10
13-Nov-20	2	3	55	43	3	9
14-Nov-20	2	4	54	34	2	10
15-Nov-20	5	0	54	31	4	6
16-Nov-20	7	2	46	35	3	4
17-Nov-20	0	3	58	19	0	2
18-Nov-20	5	1	63	46	0	1

Table A.17: Daily COVID-19 Cases by Ontario health Region, Part 5

Date	Kingston	Lambton	Leeds	Middlesex	Niagara	NorthBay
1-Oct-20	7	1	2	2	12	0
2-Oct-20	0	0	5	5	9	0
3-Oct-20	4	0	1	7	15	0
4-Oct-20	1	0	0	7	9	0
5-Oct-20	7	0	3	10	16	0
6-Oct-20	1	0	1	16	10	0
7-Oct-20	0	0	1	5	6	0
8-Oct-20	2	0	0	19	10	1
9-Oct-20	5	0	2	3	14	0
10-Oct-20	3	0	2	20	9	0
11-Oct-20	0	1	0	25	15	0
12-Oct-20	0	2	1	5	1	0
13-Oct-20	0	0	2	5	12	1
14-Oct-20	0	3	3	8	8	0
15-Oct-20	2	7	0	5	5	1
16-Oct-20	0	2	5	8	7	0
17-Oct-20	0	0	1	4	8	1
18-Oct-20	0	2	0	11	16	1
19-Oct-20	2	1	3	6	14	1
20-Oct-20	0	0	3	9	10	1
21-Oct-20	2	0	2	11	11	0
22-Oct-20	2	1	3	10	9	0
23-Oct-20	0	1	4	4	10	0
24-Oct-20	1	1	4	9	23	0
25-Oct-20	2	1	1	14	4	0
26-Oct-20	0	0	4	2	8	0
27-Oct-20	2	0	4	1	12	0
28-Oct-20	0	0	5	16	22	0
29-Oct-20	1	0	1	5	19	0
30-Oct-20	0	1	0	5	29	0
31-Oct-20	0	1	2	8	24	0
1-Nov-20	1	0	0	1	22	0
2-Nov-20	0	2	0	8	37	0
3-Nov-20	0	1	0	13	20	0
4-Nov-20	0	0	3	4	12	1
5-Nov-20	3	2	0	26	36	1
6-Nov-20	1	0	2	13	28	0
7-Nov-20	0	3	4	36	21	0
8-Nov-20	5	0	0	19	22	2
9-Nov-20	1	1	4	10	61	0

Table A.18: Daily COVID-19 Cases by Ontario health Region, Part 6

Date	Kingston	Lambton	Leeds	Middlesex	Niagara	NorthBay
10-Nov-20	3	0	1	14	26	3
11-Nov-20	1	0	1	21	15	0
12-Nov-20	2	0	2	23	27	3
13-Nov-20	6	1	3	2	12	2
14-Nov-20	10	3	2	19	19	0
15-Nov-20	6	2	0	29	23	0
16-Nov-20	3	1	1	5	19	0
17-Nov-20	5	0	1	3	27	0
18-Nov-20	3	3	1	2	9	2

Table A.19: Daily COVID-19 Cases by Ontario health Region, Part 7

Date	Northwestern	Ottawa	Peel	Peterborough	Porcupine	Waterloo
1-Oct-20	9	107	86	4	1	9
2-Oct-20	1	115	116	4	0	18
3-Oct-20	0	65	91	0	0	14
4-Oct-20	0	77	100	0	0	21
5-Oct-20	0	83	86	2	1	14
6-Oct-20	0	139	141	0	0	15
7-Oct-20	0	173	124	0	0	12
8-Oct-20	1	87	104	0	0	14
9-Oct-20	0	96	136	0	1	21
10-Oct-20	0	68	149	0	0	9
11-Oct-20	1	142	147	0	0	14
12-Oct-20	0	65	150	0	1	14
13-Oct-20	0	74	172	0	0	22
14-Oct-20	1	84	147	1	1	7
15-Oct-20	0	107	129	1	0	14
16-Oct-20	0	78	145	1	1	15
17-Oct-20	0	64	129	2	1	11
18-Oct-20	0	74	181	0	1	11
19-Oct-20	0	70	147	1	0	12
20-Oct-20	0	46	156	0	1	13
21-Oct-20	3	69	159	4	0	9
22-Oct-20	0	88	198	0	1	17
23-Oct-20	1	93	228	0	0	15
24-Oct-20	0	63	222	0	2	17
25-Oct-20	0	69	216	4	0	5
26-Oct-20	0	77	160	2	0	4
27-Oct-20	0	61	158	0	1	13
28-Oct-20	0	94	242	0	0	12
29-Oct-20	0	65	212	2	2	18
30-Oct-20	0	123	323	0	0	24
31-Oct-20	0	83	204	1	1	20
1-Nov-20	1	51	294	0	0	19
2-Nov-20	1	56	262	1	0	15
3-Nov-20	1	38	231	1	0	26
4-Nov-20	1	54	209	0	0	24
5-Nov-20	0	46	310	3	0	30
6-Nov-20	1	82	337	0	1	33
7-Nov-20	1	76	292	2	0	31
8-Nov-20	0	48	348	0	1	40
9-Nov-20	1	32	418	1	0	40

Table A.20: Daily COVID-19 Cases by Ontario health Region, Part 8

Date	Northwestern	Ottawa	Peel	Peterborough	Porcupine	Waterloo
10-Nov-20	0	53	418	5	1	53
11-Nov-20	3	49	250	0	0	28
12-Nov-20	3	91	448	4	1	58
13-Nov-20	2	41	440	1	0	43
14-Nov-20	0	77	497	5	0	67
15-Nov-20	1	62	308	3	1	48
16-Nov-20	0	51	392	6	1	67
17-Nov-20	0	11	256	1	0	42
18-Nov-20	3	22	463	0	1	54

Table A.21: Daily COVID-19 Cases by Ontario health Region, Part 9

Date	Renfrew	Simcoe	Oxford-Elgin-St. Thomas	Sudbury	ThunderBay
1-Oct-20	0	11	0	0	0
2-Oct-20	1	10	0	0	0
3-Oct-20	2	5	1	0	0
4-Oct-20	1	11	0	0	0
5-Oct-20	1	23	0	0	0
6-Oct-20	4	19	1	1	0
7-Oct-20	1	26	0	0	0
8-Oct-20	0	18	0	1	0
9-Oct-20	2	17	1	0	2
10-Oct-20	1	21	3	0	0
11-Oct-20	1	12	0	0	0
12-Oct-20	0	8	1	1	0
13-Oct-20	1	15	4	0	0
14-Oct-20	1	8	5	0	0
15-Oct-20	4	14	2	0	0
16-Oct-20	1	8	2	1	0
17-Oct-20	3	25	2	0	0
18-Oct-20	1	10	5	0	0
19-Oct-20	0	21	3	0	0
20-Oct-20	2	11	0	4	0
21-Oct-20	1	18	5	1	0
22-Oct-20	1	12	0	2	5
23-Oct-20	9	13	2	4	1
24-Oct-20	1	27	1	1	0
25-Oct-20	0	18	2	0	0
26-Oct-20	0	18	1	2	0
27-Oct-20	2	13	1	0	0
28-Oct-20	0	24	6	0	0
29-Oct-20	6	18	1	0	0
30-Oct-20	1	24	2	0	2
31-Oct-20	2	29	3	3	0
1-Nov-20	3	20	22	1	0
2-Nov-20	0	18	14	1	0
3-Nov-20	1	19	3	1	0
4-Nov-20	0	12	2	2	0
5-Nov-20	1	18	5	12	1
6-Nov-20	2	18	2	18	10
7-Nov-20	2	9	2	3	8
8-Nov-20	1	21	8	8	1
9-Nov-20	0	15	3	5	3

Table A.22: Daily COVID-19 Cases by Ontario health Region, Part 10

Date	Renfrew	Simcoe	Oxford-Elgin-St. Thomas	Sudbury	ThunderBay
10-Nov-20	0	28	18	6	1
11-Nov-20	1	13	7	4	0
12-Nov-20	0	20	14	8	1
13-Nov-20	0	27	3	6	2
14-Nov-20	2	34	9	5	5
15-Nov-20	1	26	13	6	4
16-Nov-20	6	35	10	1	4
17-Nov-20	0	19	6	1	9
18-Nov-20	0	25	14	1	20

Table A.23: Daily COVID-19 Cases by Ontario health Region, Part 11

Date	Timiskaming	Toronto	Wellington	Windsor	York
1-Oct-20	0	284	3	2	41
2-Oct-20	0	266	2	1	43
3-Oct-20	0	253	0	7	61
4-Oct-20	0	216	6	5	45
5-Oct-20	0	180	6	15	67
6-Oct-20	0	269	8	3	78
7-Oct-20	0	327	4	3	73
8-Oct-20	0	313	12	8	63
9-Oct-20	0	238	10	8	85
10-Oct-20	0	223	7	3	84
11-Oct-20	0	328	6	17	41
12-Oct-20	0	194	5	2	57
13-Oct-20	0	294	5	2	81
14-Oct-20	0	346	5	2	129
15-Oct-20	0	289	11	12	54
16-Oct-20	0	216	11	5	101
17-Oct-20	0	233	3	2	101
18-Oct-20	0	306	1	7	109
19-Oct-20	0	286	6	3	68
20-Oct-20	0	348	3	1	67
21-Oct-20	0	303	12	6	100
22-Oct-20	0	356	14	2	117
23-Oct-20	0	330	14	6	105
24-Oct-20	0	295	5	8	123
25-Oct-20	0	336	8	4	91
26-Oct-20	0	300	3	14	113
27-Oct-20	0	387	11	4	96
28-Oct-20	0	277	4	8	87
29-Oct-20	0	298	3	8	128
30-Oct-20	0	339	14	9	67
31-Oct-20	0	310	3	12	116
1-Nov-20	0	405	8	10	87
2-Nov-20	0	298	6	3	65
3-Nov-20	0	325	5	3	83
4-Nov-20	0	305	10	8	79
5-Nov-20	0	412	24	15	132
6-Nov-20	0	450	8	8	115
7-Nov-20	0	373	16	29	119
8-Nov-20	0	504	15	20	84
9-Nov-20	0	409	9	3	122

Table A.24: Daily COVID-19 Cases by Ontario health Region, Part 12

Date	Timiskaming	Toronto	Wellington	Windsor	York
10-Nov-20	0	514	12	24	178
11-Nov-20	0	100	10	23	105
12-Nov-20	0	472	14	39	155
13-Nov-20	0	440	19	17	155
14-Nov-20	0	456	5	44	130
15-Nov-20	0	364	24	23	125
16-Nov-20	1	508	14	14	170
17-Nov-20	0	569	22	16	94
18-Nov-20	0	410	23	17	178

Table A.25: Ontario Population by Health Regions

Health Region	Population
The District of Algoma	111,060
Brant County	152,029
Chatham-Kent	105,303
Durham Regional	699,641
Eastern Ontario	179,454
Grey Bruce	154,672
Haldimand-Norfolk	113,098
Haliburton, Kawartha, Pine Ridge	185,663
Halton Regional	605,475
City of Hamilton	576,272
Hastings and Prince Edward Counties	144,779
Huron Perth	136,672
Kingston Frontenac and Lennox & Addington	206,768
Lambton	115,985
Leeds Grenville and Lanark District	153,598
Middlesex-London	492,971
Niagara Region	450,816
North Bay Parry Sound District	128,804
Northwestern	74,771
City of Ottawa	1,019,693
Oxford-Elgin-St. Thomas	209,238
Peel	1,553,076
Peterborough County-City	144,237
Porcupine	90,540
Renfrew County and District	106,578
Simcoe Muskoka District	562,142
Sudbury and District	202,681
Thunder Bay District	154,444
Timiskaming	33,389
City of Toronto	2,987,513
Waterloo	571,232
Wellington-Dufferin-Guelph	304,193
Windsor-Essex County	348,836
York Regional	1,200,761